Available online at www.sciencedirect.com
ScienceDirect
Biomaterials 29 (2008) 1989–2006
Biomaterials
www.elsevier.com/locate/biomaterials

Review

Electrospinning: Applications in drug delivery and tissue engineering

Travis J. Sill, Horst A. von Recum*

Department of Biomedical Engineering, Case Western Reserve University, Cleveland, OH 44106, USA

Received 13 September 2007; accepted 9 January 2008
Available online 20 February 2008

Abstract

Despite its long history and some preliminary work in tissue engineering nearly 30 years ago, electrospinning has not gained widespread interest as a potential polymer processing technique for applications in tissue engineering and drug delivery until the last 5–10 years. This renewed interest can be attributed to electrospinning's relative ease of use, adaptability, and the ability to fabricate fibers with diameters on the nanometer size scale. Furthermore, the electrospinning process affords the opportunity to engineer scaffolds with micro to nanoscale topography and high porosity similar to the natural extracellular matrix (ECM). The inherently high surface to volume ratio of electrospun scaffolds can enhance cell attachment, drug loading, and mass transfer properties. Various materials can be electrospun including: biodegradable, non-degradable, and natural materials. Electrospun fibers can be oriented or arranged randomly, giving control over both the bulk mechanical properties and the biological response to the scaffold. Drugs ranging from antibiotics and anticancer agents to proteins, DNA, and RNA can be incorporated into electrospun scaffolds. Suspensions containing living cells have even been electrospun successfully. The applications of electrospinning in tissue engineering and drug delivery are nearly limitless. This review summarizes the most recent and state of the art work in electrospinning and its uses in tissue engineering and drug delivery.
© 2008 Elsevier Ltd. All rights reserved.

Keywords: Electrospinning; Nanofibers; Tissue engineering; Drug delivery; Gene delivery

1. Introduction

1.1. History of electrospinning

The process of using electrostatic forces to form synthetic fibers has been known for over 100 years. This process, known as electrospinning, utilizes a high voltage source to inject charge of a certain polarity into a polymer solution or melt, which is then accelerated toward a collector of opposite polarity. As the electrostatic attraction between the oppositely charged liquid and collector and the electrostatic repulsions between like charges in the liquid become stronger the leading edge of the solution changes from a rounded meniscus to a cone (the Taylor cone). A fiber jet is eventually ejected from the Taylor cone as the electric field strength exceeds the surface tension of the liquid. The fiber jet travels through the atmosphere allowing the solvent to evaporate, thus leading to the deposition of solid polymer fibers on the collector. Fibers produced using this process typically have diameters on the order of a few micrometers down to the tens of nanometers. The capacity to easily produce materials at this biological size scale has created a renewed interest in electrospinning for applications in tissue engineering and drug delivery.

While electrospinning has proven to be a relatively simple and versatile method for forming non-woven fibrous mats, a number of processing parameters can greatly influence the properties of the generated fibers. Early on, technical difficulties relating to a number of these parameters prevented electrospinning from emerging as a feasible technique for spinning small-diameter polymer fibers. It was not until 1934, when Formhals patented a process and an apparatus that used electric charges to spin synthetic fibers, that electrospinning truly surfaced as a valid technique for spinning small-diameter fibers [1]. The apparatus employed by Formhals utilized a movable

* Corresponding author. Department of Biomedical Engineering, Center for the Delivery of Molecules and Cells, Case Western Reserve University, Room 309 Wickenden Building, 10900 Euclid Avenue, Cleveland, OH 44106-7207, USA. Tel.: +1 216 368 5513; fax: +1 216 368 4969.
E-mail address: horst.vonrecum@case.edu (H.A. von Recum).

0142-9612/$ - see front matter © 2008 Elsevier Ltd. All rights reserved.
doi:10.1016/j.biomaterials.2008.01.011

thread-collecting device that collected fibers in a stretched state, allowing for the collection of aligned fibers. Using this apparatus, Formhals was able to successfully spin cellulose acetate fibers using an acetone/alcohol solution as the solvent.

While Formhals' invention did show significant improvement over earlier electrospinning methods, there still existed some disadvantages. Due to the close proximity of the collector to the charged polymer solution, the solvent could not completely evaporate before the fiber jet reached the collector, resulting in the formation of a loose web structure. Another consequence of incomplete solvent evaporation was that the fibers tended to stick to the collector as well as to each other, making removal problematic. Thus, in a second patent Formhals detailed a new process in which a greater distance was used between the spinning and collecting sites thus alleviating many of the problems seen with his earlier apparatus [2]. In his second patent, Formhals also describes the use of multiple nozzles for the simultaneous spinning of a number of fibers from the same polymer solution as well as a means to direct the fiber jets toward the collector. In 1940, Formhals patented a new process in which a polymer solution was directly electrospun onto a moving base thread to generate composite fibers [3].

Following the work of Formhals the focus turned to developing a better understanding of the electrospinning process; however, it would be nearly 30 years before Taylor would publish work regarding the jet forming process. In 1969, Taylor published his work examining how the polymer droplet at the end of a capillary behaves when an electric field is applied [4]. In his studies he found that the pendant droplet develops into a cone (now called the Taylor cone) when the surface tension is balanced by electrostatic forces. He also found that the fiber jet is emitted from the apex of the cone, which is one reason why electrospinning can be used to generate fibers with diameters significantly smaller than the diameter of the capillary from which they are ejected. Taylor subsequently determined that an angle of 49.3 degrees with respect to the axis of the cone at the cone apex (or a cone angle of 98.6 degrees) is necessary in order to balance the surface tension with the electrostatic forces by examining a variety of viscous fluids.

Shortly after Taylor's work on the jet forming process was published, interest shifted away from a fundamental understanding of the electrospinning process to a deeper understanding of the relationships between individual processing parameters and the structural properties of electrospun fibers. In 1971, Baumgarten began to investigate the affect of varying certain solution and processing parameters (solution viscosity, flow rate, applied voltage, etc.) on the structural properties of electrospun fibers [5]. In his studies, Baumgarten used a polyacrylonitrile/dimethylformamide (PAN/DMF) solution, which was ejected from a metal capillary. Using a high-speed camera he was able to determine that a single fiber was being drawn from the electrically charged pendant drop. Using this system he also discovered that fiber diameter had a direct dependence on solution viscosity, with higher viscosities giving larger fiber diameters. Furthermore, Baumgarten found that fiber diameter does not monotonically decrease with increasing applied electric field. Rather the fiber diameter decreases initially with an increase in applied field reaching a minimum and then diameter increases when the applied field is increased further. By varying the solution and processing parameters he was able to electrospin fibers with diameters ranging between 500 and 1100 nm. Approximately a decade after Baumgarten's initial work, other work began to examine electrospinning of polymer melts, which afforded new means of manipulating the structural properties of the electrospun fibers. Larrondo and Mandley were able to successfully electrospin fibers from polyethylene and polypropylene melts [6,7]. Interestingly, they found that fibers electrospun from a melt had relatively larger diameters than fibers spun from a solution. They also discovered that the fiber diameter is inversely related to the melt temperature.

Around this same time period others were beginning to examine the potential applications of electrospun fibrous mats in fields such as tissue engineering. In 1978, Annis and Bornat published work examining electrospun polyurethane mats for use as vascular prosthesis [8]. As early as 1985, Fisher and Annis were examining the long-term *in vivo* performance of an electrospun arterial prosthesis [9]. Despite these early efforts to use electrospun fibrous mats in tissue engineering applications, it would be nearly a decade before there would be widespread interest in electrospinning as a polymer processing method for applications in tissue engineering and drug delivery.

1.2. Electrospinning process

The process of electrospinning, namely utilizing electrostatic forces to generate polymer fibers, traces its roots back to the process of electrospraying, in which solid polymer droplets are formed rather than fibers. In fact, a number of processing parameters must be optimized in order to generate fibers as opposed to droplets, and a typical electrospinning apparatus can be used to form fibers, droplets, or a beaded structure depending on the various processing parameters, such as distance between source and collector. In recent work, a greater understanding of processing parameters has led to the formation of fibers with diameters in the range of 100–500 nm, typically referred to as nanofibers. The development of nanofibers has led to resurgence in interest regarding the electrospinning process due to potential applications in filtration, protective clothing, and biological applications such as tissue engineering scaffolds, and drug delivery devices.

A typical electrospinning setup consists of a capillary through which the liquid to be electrospun is forced; a high voltage source with positive or negative polarity, which injects charge into the liquid; and a grounded collector (Fig. 1). A syringe pump, gravitational forces, or pressurized gas are typically used to force the liquid through a small-diameter capillary forming a pendant drop at the tip. An electrode from the high voltage source is then immersed in the liquid or can be directly attached to the capillary if a metal needle is used. The voltage source is then turned on and charge is injected into the polymer solution. Increasing the electric field

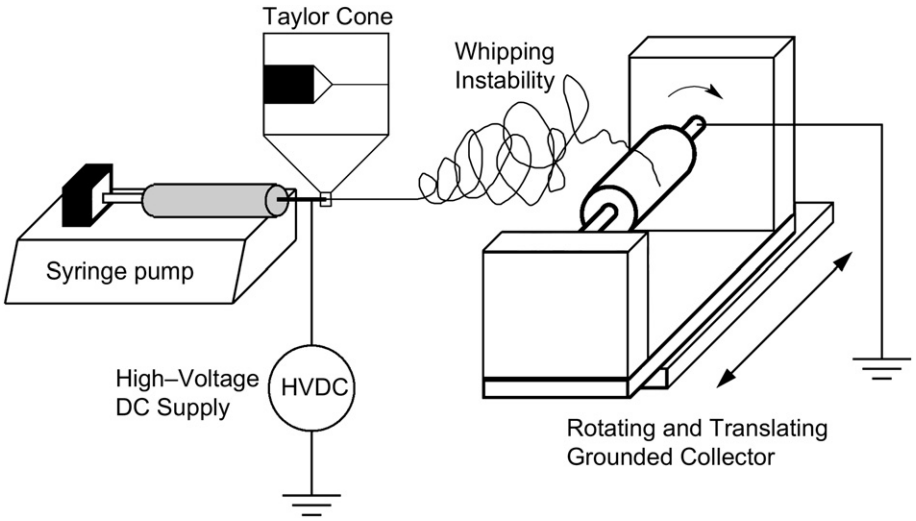

Fig. 1. Schematic of a typical electrospinning system. A polymer solution is forced through a needle using a syringe pump. The needle is connected to a high voltage DC supply, which injects charge of a certain polarity into the polymer solution. If the electrostatic force created by the repulsion of similar charges is sufficient to overcome the surface tension of the polymer solution the Taylor cone is formed and a fiber jet is emitted from its apex. While the fiber jet is traveling toward the grounded collector it undergoes a chaotic whipping instability. The fiber jet is then deposited on the collector, which can be rotating and translating as depicted here.

strength causes the repulsive interactions between like charges in the liquid and the attractive forces between the oppositely charged liquid and collector to begin to exert tensile forces on the liquid, elongating the pendant drop at the tip of the capillary. As the electric field strength is increased further a point will be reached at which the electrostatic forces balance out the surface tension of the liquid leading to the development of the Taylor cone. If the applied voltage is increased beyond this point a fiber jet will be ejected from the apex of the cone and be accelerated toward the grounded collector.

While the fiber jet is accelerated through the atmosphere toward the collector it undergoes a chaotic bending instability, thereby increasing the transit time and the path length to the collector and aiding in the fiber thinning and solvent evaporation processes. Yarin et al. have suggested that this bending instability is due to repulsive interactions between like charges found in the polymer jet [10]. Doshi and Reneker had hypothesized that charge density increases as the fiber jet thins, dramatically increasing radial charge repulsion which causes the fiber jet to split into a number of smaller fibers when a critical charge density is met [11]. However, in more recent studies high-speed photography has been used to image the unstable zone of the fiber jet, revealing that a whipping instability causes the single fiber to bend and turn rapidly giving the impression that the fiber is splitting [12,13].

The solid polymer fibers are then deposited onto a grounded collector. Depending on the application a number of collector configurations can be used, including a stationary plate, rotating mandrel, solvent (e.g. water), etc. Typically the use of a stationary collector will result in the formation of a randomly oriented fiber mat. A rotating collector can be used to generate mats with aligned fibers, with the rotation speed playing an important role in determining the degree of anisotropy. Additionally, Liu and Hsieh found that both the conductivity and the porosity of the collector play an important role in determining the packing density of the collected fibers [14]. Electrospun cellulose acetate fibers were collected using copper mesh, aluminum foil, water, and paper. The authors found that non-conductive collectors yielded a more porous structure. They hypothesized that conductive collectors are able to dissipate the residual charge of the fibers, while non-conductive collectors lack this ability causing the collected fibers to repel each other, thus decreasing the packing density. Additionally the authors found that more porous collectors resulted in a lower fiber packing density. Furthermore, the geometry of the collector can be selected based on the application so as to form either a sheet or a tubular construct from the same electrospinning setup merely by changing the collector. For example, a 2-dimensional copper mesh can be used to form a sheet, while a cylindrical, rotating mandrel can be used to form a tubular scaffold. This ease of use and adaptability is one of the main reasons for electrospinning's renewed popularity.

1.3. Processing parameters

Despite electrospinning's relative ease of use, there are a number of processing parameters that can greatly affect fiber formation and structure. Grouped in order of relative impact to the electrospinning process, these parameters are applied voltage, polymer flow rate, and capillary-collector distance. Furthermore, all three parameters can influence the formation of bead defects.

1.3.1. Applied voltage

The strength of the applied electric field controls formation of fibers from several microns in diameter to tens of nanometers. Suboptimal field strength could lead to bead defects in the spun fibers or even failure in jet formation. Deitzel et al.

examined a polyethylene oxide (PEO)/water system and found that increases in applied voltage altered the shape of the surface at which the Taylor cone and fiber jet were formed [15]. At lower applied voltages the Taylor cone formed at the tip of the pendent drop; however, as the applied voltage was increased the volume of the drop decreased until the Taylor cone was formed at the tip of the capillary, which was associated with an increase in bead defects seen among the electrospun fibers (Fig. 2).

Meechaisue et al. examined the affects of various solution and processing parameters, including applied electric field strength, on the morphology of electrospun poly(desaminotyrosyl-tyrosine ethyl ester carbonate) (poly(DTE carbonate)) [16]. The authors examined the affect of varying the applied electric field strength from 10 to 25 kV/10 cm for two poly(DTE carbonate) solutions with polymer concentrations of 15 and 20% (w/v). For the 15% (w/v) poly(DTE carbonate) solution the authors observed primarily beaded fibers when the applied electric field strength was below 20 kV/10 cm, while mostly smooth fibers were obtained above this field strength. Increasing the electric field strength from 10 to 15 kV/10 cm decreased the bead density, while increasing the field strength from 20 to 25 kV/10 cm increased the average fiber diameter from 1.9 to 2.2 μm. The authors attribute the increase in fiber diameter to the increase in the mass flow rate relative to the increase in the electrostatic force. For the 20% (w/v) poly(DTE carbonate) solution only smooth fibers were obtained at all electric field strengths. Additionally, the average fiber diameter was found to increase monotonically from about 2.5 μm at 10 kV/10 cm to about 5.4 μm at 25 kV/10 cm, while the fiber density monotonically decreased over this same range. Based on the work by Deitzel et al., Meechaisue et al. and others it is evident that there is an optimal range of electric field strengths for a certain polymer/solvent system, as either too weak or too strong a field will lead to the formation of beaded fibers.

1.3.2. Flow rate

Polymer flow rate also has an impact on fiber size, and additionally can influence fiber porosity as well as fiber shape.

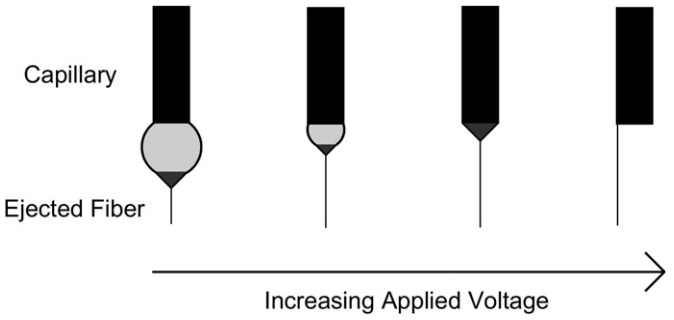

Fig. 2. Effect of varying the applied voltage on the formation of the Taylor cone. At relatively low applied voltages a pendant drop (depicted in light gray) is formed at the tip of the capillary. The Taylor cone (depicted in dark gray) then forms at the tip of the pendant drop. However, as the applied voltage is increased (moving from left to right) the volume of the pendant drop decreases until the Taylor cone is formed at the tip of the capillary. Increasing the applied voltage further results in the fiber jet being ejected from within the capillary, which is associated with an increase in bead defects.

As a result of his work, Taylor realized that the cone shape at the tip of the capillary cannot be maintained if the flow of solution through the capillary is insufficient to replace the solution ejected as the fiber jet [4]. Megelski et al. examined the effects of flow rate on the structure of electrospun fibers from a polystyrene/tetrahydrofuran (THF) solution [17]. They demonstrated that both fiber diameter and pore size increase with increasing flow rate. Additionally, at high flow rates significant amounts of bead defects were noticeable, due to the inability of fibers to dry completely before reaching the collector. Incomplete fiber drying also leads to the formation of ribbon-like (or flattened) fibers as compared to fibers with a circular cross section.

1.3.3. Capillary − collector distance

While playing a much smaller role, the distance between capillary tip and collector can also influence fiber size by 1−2 orders of magnitude. Additionally, this distance can dictate whether the end result is electrospinning or electrospraying. Doshi and Reneker found that the fiber diameter decreased with increasing distances from the Taylor cone [11]. In another study, Jaeger et al. electrospun fibers from a PEO/water solution and examined the fiber diameter as a function of the distance from the Taylor cone [18]. They found that the diameter of the fiber jet decreased approximately 2-fold, from 19 to 9 μm after traveling distances of 1 and 3.5 cm, respectively. Additionally, Megelski et al. were able to notice the formation of a beaded morphology for electrospun polystyrene fibers upon shortening of the distance between the capillary tip and the collector, which can be attributed to inadequate drying of the polymer fiber prior to reaching the collector [17].

1.4. Solution parameters

In addition to the processing parameters a number of solution parameters play an important role in fiber formation and structure. In relative order of their impact on the electrospinning process these include polymer concentration, solvent volatility and solvent conductivity.

While a number of general relationships between processing parameters and fiber morphology can be drawn (Table 1),

Table 1
Effects of electrospinning parameters on fiber morphology

Parameter	Effect on fiber morphology
Applied voltage ↑	Fiber diameter ↓ initially, then ↑ (not monotonic)
Flow rate ↑	Fiber diameter ↑ (beaded morphologies occur if the flow rate is too high)
Distance between capillary and collector ↑	Fiber diameter ↓ (beaded morphologies occur if the distance between the capillary and collector is too short)
Polymer concentration (viscosity) ↑	Fiber diameter ↑ (within optimal range)
Solution conductivity ↑	Fiber diameter ↓ (broad diameter distribution)
Solvent volatility ↑	Fibers exhibit microtexture (pores on their surfaces, which increase surface area)

it is important to realize that the exact relationship will differ for each polymer/solvent system. Depending on a number of solution parameters very different results can be obtained using the same polymer and electrospinning setup. Thus, it is difficult to give quantitative relationships that can be applied across a broad range of polymer/solvent systems. This being said, there are general trends which are useful when determining the optimum conditions for a certain system.

1.4.1. Polymer concentration

The polymer concentration determines the spinnability of a solution, namely whether a fiber forms or not. The solution must have a high enough polymer concentration for chain entanglements to occur; however, the solution cannot be either too dilute or too concentrated. The polymer concentration influences both the viscosity and the surface tension of the solution, both of which are very important parameters in the electrospinning process. If the solution is too dilute then the polymer fiber will break up into droplets before reaching the collector due to the effects of surface tension. However, if the solution is too concentrated then fibers cannot be formed due to the high viscosity, which makes it difficult to control the solution flow rate through the capillary. Thus, an optimum range of polymer concentrations exists in which fibers can be electrospun when all other parameters are held constant. Doshi and Reneker, electrospun fibers from PEO/water solutions containing various PEO concentrations and found that solutions with viscosity less than 800 centipoises broke up into droplets upon electrospinning while solutions with viscosity greater than 4000 centipoises were too thick to electrospin [11]. In many experiments it has been shown that within the optimal range of polymer concentrations fiber diameter increases with increasing polymer concentration (Fig. 3). Megelski et al. found that by increasing the concentration of polystyrene in THF the fiber diameter increased and the distribution of pore sizes became narrower [17]. Deitzel et al. found that fiber diameter of fibers electrospun from PEO/water solution were related to PEO concentration by a power law relationship [15].

1.4.2. Solvent volatility

Choice of solvent is also critical as to whether fibers are capable of forming, as well as influencing fiber porosity. In order for sufficient solvent evaporation to occur between the capillary tip and the collector a volatile solvent must be used. As the fiber jet travels through the atmosphere toward

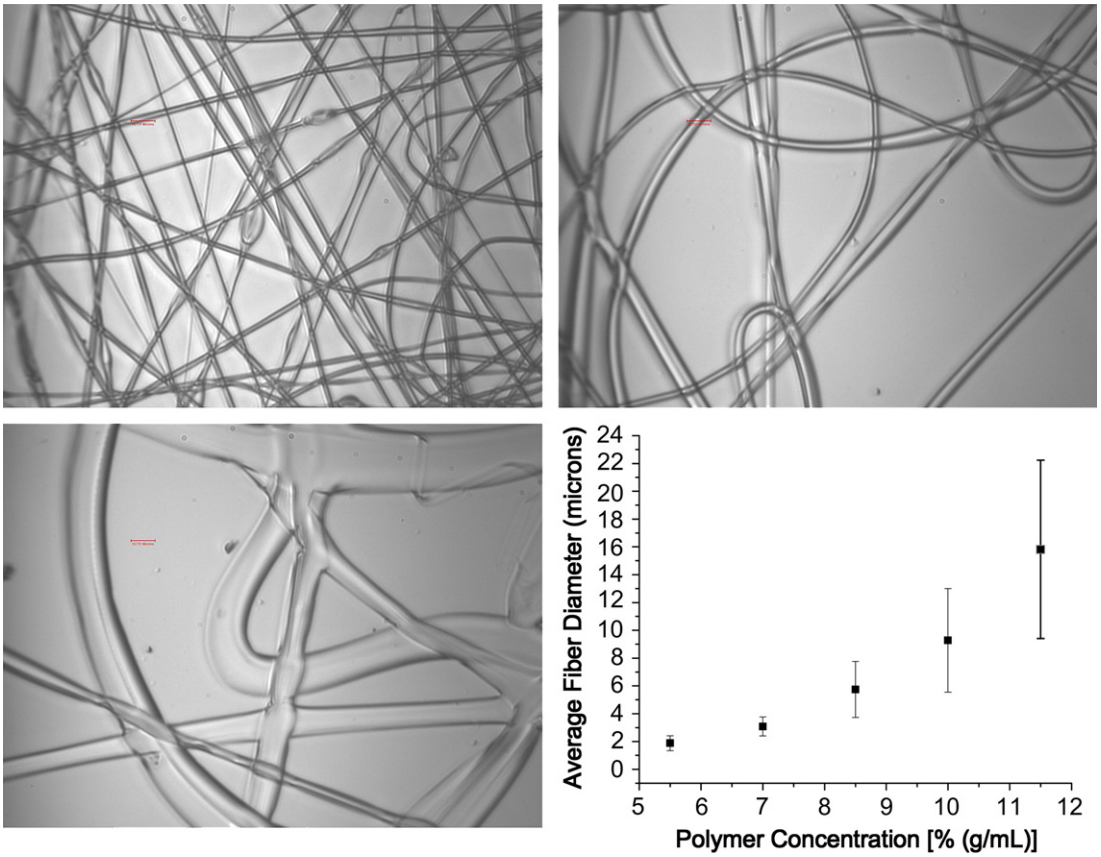

Fig. 3. Effect of polymer concentration on fiber diameter. Fibers were electrospun from solutions containing varying concentrations of poly(ethylene-*co*-vinyl alcohol) in 70:30 (v:v) 2-propanol: DI water. Top left: Fibers electrospun from a 5.5% (g/mL) solution. Top right: Fibers electrospun from an 8.5% (g/mL) solution. Bottom left: Fibers electrospun from an 11.5% (g/mL) solution. The following processing parameters were used for all experiments: applied voltage: 20 kV (+polarity), flow rate: 3 mL/h, capillary-collector distance: approximately 25 cm. In the bottom right panel the relationship between the average fiber diameter and the polymer concentration is given. Note that the mean fiber diameter increases monotonically with increasing polymer concentration. Additionally, it is evident that ribbon-like fibers are formed at higher concentrations (11.5%), which indicates incomplete polymer drying. (Error bars represent the standard deviation.).

the collector a phase separation occurs before the solid polymer fibers are deposited, a process that is greatly influenced by the volatility of the solvent. Megelski et al. examined the structural properties of polystyrene fibers electrospun from solutions containing various ratios of DMF and THF [17]. Solutions electrospun from 100% THF (more volatile) demonstrated a high density of pores, which increased the surface area of the fiber by as much as 20–40% depending on the fiber diameter. Solutions electrospun from 100% DMF (less volatile) demonstrated almost a complete loss of microtexture with the formation of smooth fibers. Between these two extremes it was observed that pore size increased with decreased pore depth (thus decreasing pore density) as the solvent volatility decreased. As mentioned previously a phase separation occurs as the polymer jet is traveling through the atmosphere. This phase separation can be vapor-induced, which occurs when non-solvent from the vapor phase penetrates the polymer solution [17]. However, transport of the non-solvent into the polymer solution is limited by the slow diffusion of the non-solvent adjacent to the fiber surface. For very volatile solvents, the region adjacent to the fiber surface can be saturated with solvent in the vapor phase, which further limits the penetration of non-solvent. This can hinder skin formation leading to the development of a porous surface morphology.

1.4.3. Solution conductivity

Solution conductivity, while playing a lesser role, can influence fiber size within 1–2 orders of magnitude. Solutions with high conductivity will have a greater charge carrying capacity than solutions with low conductivity. Thus the fiber jet of highly conductive solutions will be subjected to a greater tensile force in the presence of an electric field than will a fiber jet from a solution with a low conductivity. As would be expected, Baumgarten was able to show that the radius of the fiber jet is inversely related to the cube root of the solution conductivity [5]. Hayati et al. were able to show that highly conductive solutions were extremely unstable in the presence of strong electric fields, which led to a dramatic bending instability as well as a broad diameter distribution [19]. However, semi-conducting and insulating liquids such as paraffinic oil produced relatively stable fibers. Zhang et al. examined the affect of adding ions to PVA/water solution on the diameters of electrospun fibers [20]. By adding increasing concentrations of NaCl (ranging from 0.05 to 0.2%) to the PVA/water solution, the authors were able to decrease the mean fiber diameter from 214 ± 19 nm to 159 ± 21 nm. The authors attribute this decrease in the mean fiber diameter to the increased net charge density imparted by the NaCl, which increased the electric force exerted on the jet. The authors also determined that the solution conductivity increased from 1.53 to 10.5 mS/cm by increasing the NaCl concentration from 0.05 to 0.2%, further strengthening their observations. Jiang et al. examined whether or not bovine serum albumin (BSA) could be directly incorporated into electrospun dextran fibers for potential drug delivery or tissue engineering applications [21]. They observed that adding 5% BSA decreased the mean fiber diameter from approximately 2.5 μm–500 nm. However, the viscosity of the dextran solution was unchanged by the addition of up to 10% BSA, indicating that the decrease in fiber diameter was due to the increased net charge found in the polymer jets.

1.5. Types of electrospinning

In addition to adjusting solution or processing parameters, the type of electrospinning process can greatly influence the resulting product. This can include choices in nozzle configuration (single, single with emulsion, side-by-side, or coaxial nozzles), or solution vs. melt spinning.

1.5.1. Nozzle configuration

Depending on the application a number of nozzle configurations have been employed. Perhaps the simplest and most common configuration is the single nozzle technique. In this configuration a charged polymer solution flows through a single capillary (Fig. 1). This configuration is very versatile and has been used to electrospin single polymer solutions [22] as well as polymer blends out of polymers soluble in a common solvent [23]. As an example, Qi et al. used a single nozzle configuration with an emulsion to electrospin composite fibers containing bovine serum albumin (BSA) loaded Ca-alginate microspheres microencapsulated in poly(L-lactic acid) (PLLA) fibers [24].

While electrospinning polymer blends is often desirable in order to achieve the desired combination of properties, it may not be possible using a single needle configuration if the polymers of interest are not soluble in a common solvent. Thus, it may be necessary to use a side-by-side configuration. In this configuration two separate polymer solutions flow through two different capillaries, which are set side-by-side (Fig. 4). Gupta and Wilkes used a side-by-side configuration to electrospin bicomponent systems out of poly(vinyl chloride)/segmented polyurethane and poly(vinyl chlorine)/poly(vinylidiene fluoride) [25]. They observed that the solution conductivity plays a more important role in the ability to form a single fiber jet under a strong electric field in the side-by-side configuration. The conductivity of the PVC solution was significantly higher than either of the other two solutions, and thus two distinct Taylor cones, one from each solution, were formed when subjected to a strong electric field. The authors also demonstrated that the ratio of the two components varies along the length of the fiber, which they attributed to fluctuations of the jet on the surface of the Taylor cone.

A relatively new nozzle configuration is the coaxial configuration, which allows for the simultaneous coaxial electrospinning of two different polymer solutions. In this configuration two separate polymer solutions flow through two different capillaries, which are coaxial with a smaller capillary inside a larger capillary (Fig. 4). This technique has received great interest as of late due to its potential in drug delivery applications [26–33]. Using this nozzle configuration a smaller fiber can essentially be encapsulated in a larger fiber leading to what is known as a core-shell morphology. Using a coaxial configuration, Townsend-Nicholson and Jayasinghe have demonstrated the successful encapsulation of living cells within

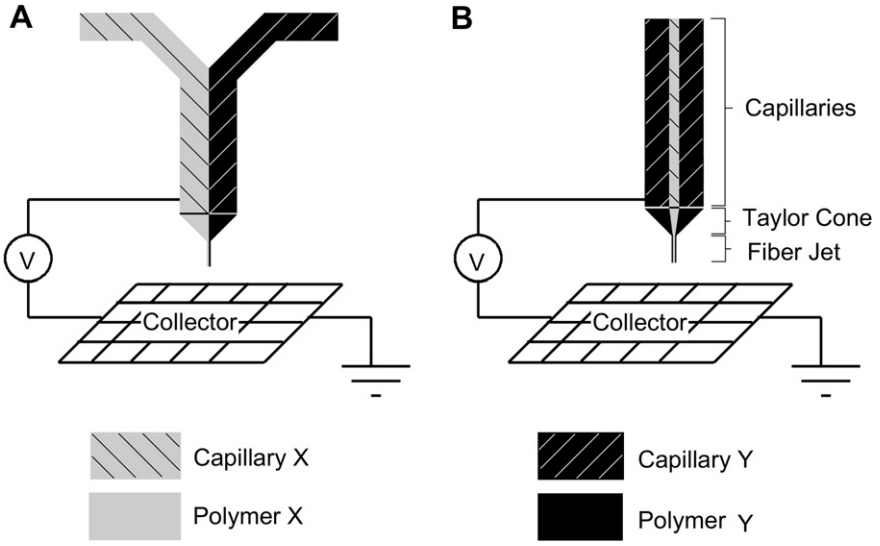

Fig. 4. (A) Schematic of side-by-side nozzle configuration. Two capillaries containing different polymer solutions are set side-by-side. As long as the two solutions have similar conductivities a single Taylor cone will be developed and a fiber jet containing both polymers will be produced. However, the relative amounts of each polymer can vary along the electrospun fiber. (B) Schematic of coaxial nozzle configuration. A smaller capillary is set inside a larger capillary such that the long axes of the capillaries coincide. Different polymer solutions are passed through each capillary. At the tip of the capillaries the Taylor cone is formed and leads to the formation of fibers in which one polymer fiber is encapsulated within another (known as a core-shell morphology).

a poly(dimethylsiloxane) (PDMS) fiber [29]. Cell viability throughout the process remained high, with approximately $67.6 \pm 1.9\%$ cells surviving the electrospinning process as compared to $70.6 \pm 5.0\%$ for control cells. Additionally, electrospun cells were reported to show no observable difference in cell morphology or rate of growth between the electrospun and control cells over the evaluated time period (6 days). While the authors have demonstrated the feasibility of electrospinning living biosuspensions, more work is needed before the true efficacy of such a technique for tissue engineering applications can be determined, including preventing the loss of cell encapsulation almost immediately after electrospinning, maintaining long-term viability, as well as evaluating nutrient and waste transport, and if relevant, degradation characteristics.

In a drug delivery application, Zhang et al. demonstrated encapsulation of a model protein, fluorescein isothiocyanate-conjugated bovine serum albumin, along with poly(ethylene glycol) (PEG) in poly(ϵ-caprolactone) (PCL) fibers by using a coaxial configuration [28]. The authors were able to demonstrate that the resulting core-shell system greatly mitigated the initial burst release associated with release from polymer/drug blends, and had longer sustained release.

1.5.2. Solution vs. melt electrospinning

When electrospinning a polymer, typically one of two methods can be used. The polymer can be dissolved in a suitable solvent and electrospun or the polymer can be directly electrospun from a melt. In general, solution spinning results in a greater range of fiber sizes, while melt spun fibers are typically limited to micron size or larger [6,7], however, there are specific advantages and disadvantages to each method. Melt electrospinning eliminates the need for harsh organic solvents, which is ideal for scaled-up processes. However, melts must be kept at elevated temperatures to be electrospun; whereas, stable solutions can typically be electrospun at room temperature. Dalton et al. examined the melt electrospinning of block copolymers of PEG and PCL at various molecular weights, and determined that the optimum melt temperatures ranged between 60 and 90 °C [34]. These higher temperatures may preclude their use for tissue engineering or drug delivery applications. Using polymer melts also eliminates the problem of inadequate solvent evaporation between the capillary tip and the collector; however, the polymer must be able to cool sufficiently over this distance in order to generate fibers with a cylindrical morphology.

1.6. Electrospun fiber properties

The capacity to adjust fiber size is one of the strengths of electrospinning since fibers with diameters in the nanometer size range closely mimic the size scale of fibrous proteins found in the natural extracellular matrix (ECM), such as collagen. This ability of electrospun nanofibers to mimic the ECM is vital as previous studies have shown that both the size scale of the structure and the topography play important roles in cell proliferation and adhesion, respectively [35–37]. Also, nonwoven fibrous mats comprised of nanofibers have a very high fraction of surface available to interact with cells, which make them ideal for cell attachment [38,39]. Additionally, the porosity of electrospun mats aids in nutrient transport. However, many researches have encountered limitations with regards to cell infiltration into nanofiber mats due to the relatively small pores associated with such matrices. In order to combat these limitations researchers have been examining possible ways to engineer nanofiber mats with pores of

a desired size, which would aid in cell infiltration and angiogenesis allowing for incorporation of the nanofiber scaffold into the surrounding tissue (see section 2.1.3).

While this review has primarily focused on the capacity to change fiber size, there are a number of other physical properties which can be optimized and which play a critical role in tissue engineering and drug delivery applications. This includes the development of beaded and core-shell structures, which can potentially act as drug reservoirs, with ability to mitigate the initial burst release as well as provide sustained release. Nanofibrous mats have the potential to overcome mass transfer limitations seen in other polymer drug delivery systems due to their high surface to volume ratio. Additionally, nanofiber systems can afford greater drug loading as compared to other comparable techniques.

In addition to these physical properties, chemical properties, including degradation rate, and mechanical properties should also be considered when optimizing electrospinning processes.

2. Applications

2.1. Tissue engineering

Use of electrospun fibers and fiber meshes in tissue engineering applications often involves several considerations, including choice of material, fiber orientation, porosity, surface modification and tissue application. Choices in materials include both natural and synthetic (biodegradable and non-degradable) materials, as well as hybrid blends of the two, which can provide an optimal combination of mechanical and biomimetic properties. By varying the previously discussed processing and solution parameters the fiber orientation (aligned vs. random) and porosity/pore size (cell infiltration) of the electrospun scaffold can be controlled and optimized for each individual application. After fabrication the surface of the scaffold can be modified with a high density of bioactive molecules due to the relatively high scaffold surface area. Due to the flexibility in material selection as well as the ability to control the scaffold properties, electrospun scaffolds have been employed in a number of different tissue applications including: vascular, bone, neural, and tendon/ligament.

2.1.1. Materials

When choosing a material for a tissue engineering application it must meet a number of requirements. Most importantly the material must be biocompatible, meaning that it induces an appropriate response in the host organism. The requirements of this response will vary from application to application; however, toxicity, as well as inflammatory and possibly immune responses should typically be minimized. Initial research in biocompatibility relied upon the use of bioinert materials, which attempted to reduce host specific interactions. While processes such as protein adsorption and the inflammatory response will occur to some degree with any implant, a bioinert material will form no (or very little) specific interactions with the surrounding environment, including the extracellular fluid or surrounding tissues. Conversely, current research has been investigating the incorporation of bioactive materials which can intentionally interact with the biological environment and influence such things as cell function [40]. These interactions are often accomplished through surface modifications allowing a large variety of synthetic, natural, or hybrid materials to be used for electrospinning.

Within the subdivision of synthetic materials one can further delineate between biodegradable and non-degradable materials. Biodegradable materials have been the more popular choice due to the elimination of a second surgery to remove the implanted scaffold [26,41–53]. Additionally, the rate of degradation can be controlled to some extent to coincide with the rate of new tissue formation, by altering parameters such as polymer blends, and ratio of amorphous to crystalline segments. Kim et al. demonstrated that the degradation rate (via hydrolysis) of blends containing different ratios of PLA, PLGA, PLA-b-PEG-b-PLA, and free lactide could be controlled by varying the blend composition (thus altering the hydrophobicity/hydrophilicity) using an *in vitro* study [53]. Henry et al. developed and characterized a slowly degrading biodegradable polyesterurethane, which they electrospun for use as a tissue engineering scaffold [45]. The authors found that by varying the relative amounts of the crystalline and amorphous segments making up the polyesterurethane, as well as the chemical composition of the amorphous segment, they could control both the mechanical properties and the degradation rate (via hydrolysis) of the scaffolds.

In addition to evaluating the degradation rate, the authors also characterized changes in mechanical properties, molecular weight, surface morphology and cell interactions by conducting an acellular, *in vitro* degradation study over a period of 12 months using electrospun polyesterurethane (fiber diameter: 3–10 μm, pore size: 10–100 μm). The ultimate tensile strength decreased from an initial value of approximately 0.29 km to a value of approximately 0.03 km (an approximate 90% decrease) over the 12-month period, while over the same period the modulus of elasticity decreased from an initial value of approximately 19 km to a value of approximately 12 km (an approximate 41% decrease). It is important to note that the reported values for the ultimate tensile strength and the modulus of elasticity are given in units of kilometers. This is in accordance with the units that are reported for textiles, and takes into account the fact that the electrospun meshes have porous cross-sectional areas [45]. However, other studies (utilizing different polymer systems) that have not used this method have reported electrospun meshes with ultimate tensile stresses and moduli of elasticity on the order of MPa [54]. During the *in vitro* degradation study the elongation to break also decreased from an initial value of approximately 470% to a value of approximately 20% (an approximate 95% decrease) over the 12-month period. The molecular weight of the electrospun mesh decreased by 70% over the 12-month period. As the degradation period progressed micropores appeared in the electrospun fibers, altering the surface morphology. Furthermore, the diameters of the fibers decreased over the course of the degradation period. 3T3

fibroblasts displayed an elongated bipolar morphology on the electrospun mesh and were viable after 7 days of culturing *in vitro*, demonstrating that the novel polyesterurethane was not cytotoxic. While studies such as this stress the importance of determining the degradation kinetics and mechanical properties of a scaffold electrospun out of a biodegradable material, future work should examine these properties in greater detail. It is imperative that the rate of degradation coincide with the rate of new tissue formation. If the rate of degradation is too slow then new tissue formation will be impeded; however, if the rate of degradation is too fast then the mechanical stability of the scaffold/developing tissue will be compromised. Additionally, degradation studies *in vivo* or at least in cell culture must be conducted before any real conclusions regarding the material's degradation profile can be drawn. A non-cellular degradation study examining the rate of hydrolysis of a material is quite different from a study in which cells are attached to the matrix and are able to secrete enzymes capable of degrading the scaffold.

Despite the popularity and apparent benefits of using biodegradable materials some research has examined the use of non-degradable materials for applications in tissue engineering [55,56]. Kenawy et al. successfully electrospun poly(ethylene-*co*-vinyl alcohol) (EVOH) fibrous mats from 70% isopropanol/water solution (rubbing alcohol) [56]. Furthermore, they were able to demonstrate that these mats supported culturing of smooth muscle cells and fibroblasts *in vitro*.

In order to more accurately mimic the natural ECM, research has also examined the electrospinning of natural materials such as: collagen [57,58], chitosan [59], gelatin [60,61], fibrinogen [62], chitin [63], and hyaluronic acid [64]. However, these materials often lack the desired physical properties or are difficult to electrospin on their own, which has led to the development of hybrid materials, which consist of a blend of synthetic and natural materials [23,65–74]. Stitzel et al. examined the use of a hybrid blend of type I collagen (45%), PLGA (40%), and elastin (15%) to form a vascular prosthesis via electrospinning [23]. The addition of PLGA was shown to improve mechanical properties such as burst strength and compliance of the prosthesis as compared to scaffolds composed solely of type I collagen and elastin (which are both components of the natural ECM of blood vessel walls). The burst pressure of the PLGA-containing prosthesis was determined to be approximately 1425 mmHg, or nearly 12 times systolic pressure. Within the physiological pressure range the diameter change was approximately 9% for native vessels and approximately 12–14% for electrospun scaffolds, demonstrating that the electrospun scaffolds have compliance similar to that of native vessels. Thus, by using a hybrid blend of materials the authors were able to produce a scaffold possessing tissue composition and mechanical properties similar to native vessels. Park et al. examined the generation of novel biodegradable scaffolds by electrospinning a hybrid blend consisting of PGA and chitin [71]. Chitin has structural characteristics similar to glycosaminoglycans (GAGs) found in the native ECM, and has antithrombogenic and wound healing properties that make its incorporation into electrospun scaffolds desirable [75]. Additionally, chitin is more hydrophilic than PGA and does not undergo degradation via hydrolysis as does PGA. Park et al. observed that the degradation rate increased with increasing chitin content [71]. They hypothesized that increases in the content of hydrophilic chitin resulted in greater hydration of the matrix leading to more rapid hydrolysis of the ester bonds located in the PGA monomers. Thus, incorporation of chitin in PGA matrices effectively accelerates degradation and can effectively be used to control the degradation rate of PGA/chitin scaffolds.

2.1.2. Fiber orientation

By using a stationary or rotating collector either randomly oriented or aligned fibers can be formed, respectively. The degree of anisotropy within an electrospun fibrous mat can greatly affect not only the mechanical properties but also cell adhesion, proliferation, and alignment. In many applications it is desirable to develop an aligned fibrous mat [42,44,48,49,52,55,61,76,77]. For example, in designing scaffolds meant to replace highly oriented tissue such as the medial layer of a native artery it is desirable to generate aligned fibrous mats. In the medial layer both smooth muscle cells and ECM fibrils are aligned circumferentially, which allows for vasoconstriction and vasodilation in response to corresponding stimuli. Xu et al. developed an aligned nanofibrous scaffold via electrospinning of a poly(L-lactate-*co*-ϵ-caprolactone) (P(LLA-CL)) (75:25) copolymer [52]. Using tissue culture polystyrene and solvent cast P(LLA-CL) films as controls, the interaction of human coronary artery smooth muscle cells with the various materials was examined *in vitro*. Smooth muscle cells attached and migrated along the axis of the aligned fibers (fiber diameter: 550 ± 120 nm). Furthermore, the proteins comprising the cytoskeleton of the smooth muscle cells were aligned parallel to the aligned fibers, demonstrating the cells proclivity to organize along oriented fiber topography. Additionally, smooth muscle cells were shown to have improved adhesion and proliferation on the aligned nanofibrous scaffold as compared to the plane polymer films. Schnell et al. examined the ability of aligned nanofibrous scaffolds to direct axonal outgrowth and glial cell migration in peripheral nerve regeneration [42]. In this study PCL and collagen/PCL nanofibrous scaffolds were produced via electrospinning. While both scaffolds were found to support oriented outgrowth of axons and glial cell migration, the collagen/PCL blend was found to give superior guidance of axons. These experiments demonstrate potential applications in which it is desirable to develop a nanofibrous scaffold containing aligned fibers (with a high degree of anisotropy).

2.1.3. Porosity/pore size

Not only the density of pores but also fiber mat pore size can play an important role in the ability of a cell to migrate and infiltrate an electrospun scaffold. Depending on the polymer/solvent system used and the various processing parameters a number of different pore sizes can be obtained. By using a theoretical model, Eichhorn and Sampson were able to analyze how the mean pore radius is affected by

such structural properties as fiber width and fiber density [78]. Utilizing a fiber density range of 0.9–1.7 g cm^{-3} and a porosity range of 0.7–0.9 they were able to examine pore sizes for typical nanofiber meshes prepared for tissue engineering applications. Using this model they were able to show that a mesh comprised of fibers with diameters of approximately 100 nm and a porosity of 80% will have pores with a mean radius on the order of 10 nm for a given fiber and areal density. Interestingly, the authors also demonstrated that for a given areal density and porosity, the mean pore radius increases with increasing fiber width. Such a finding produces an interesting paradox. A great deal of research has focused on developing fibers with ever smaller diameters, with the aim of increasing surface area; however, decreasing the fiber diameter for a given areal density and porosity will greatly limit the ability of cells to infiltrate the scaffold material. Thus, a nanofiber mesh (with fiber diameters less than 100 nm) will essentially behave as a 2-dimensional sheet on which cells are able to migrate along the surface, rather than a 3-dimensional scaffold that cells are capable of infiltrating. Indeed, as Eichhorn and Sampson mention, electrospun scaffolds are not truly 3-dimensional structures as the fiber axes may be inclined only a few degrees with respect to the plane of the network. Rather, such scaffolds can be thought of as layers of 2-dimensional networks stacked upon one another, with the overall scaffold thickness dependent upon the number of layers. However, it is important to note that areal density increases with an increasing number of layers, which will drastically reduce the mean pore radius.

Initially, small pore size was seen as a hindrance in many situations; however, it can actually serve as an advantage in applications where cell infiltration is unwanted. Round cells with diameters on the order of 10 μm cannot fit in nanofiber meshes with pores on the nanometer scale, making these meshes particularly useful for barrier applications such as skin and the endothelium. Due to this barrier property interest in electrospun scaffolds for applications in tissue engineered vascular grafts has grown significantly. An electrospun nanofiber scaffold can provide superior endothelial cell attachment due to the large fraction of surface available for interacting with cells. Additionally, due to its small pores the same scaffold can prevent smooth muscle cell migration into the lumen of the vessel, while still allowing sufficient transport for nutrients and waste removal. A tissue engineered vascular graft is one area where a 2-dimensional scaffold is ideal. While the majority of the natural extracellular matrix is 3-dimensional, the basal laminae that line all epithelial cell sheets and tubes are essentially 2-dimensional mats with a thickness on the order of 100 nm. As is the case with the basal lamina, the 2-dimensional nanofiber scaffold can act as a selective barrier to the movement of cells, allowing for the formation of a confluent endothelium while preventing intimal hyperplasia. Pore size can also be modified to allow for selective filtration of macromolecules, which can be used to control transport of nutrients and waste products.

However, small pores are not advantageous for all applications. In more 3-dimensional scaffolds the cells must be able to infiltrate deep into the scaffold, which requires pores of adequate size (approximately 10 μm) to allow for cell migration. Li et al. were able to electrospin highly porous (approximately 92%) nanofiber meshes composed of PLGA with a pore diameter distribution ranging from 2 to 465 μm [54]. These meshes were composed of fibers with diameters between 500 and 800 nm. BALB/c C7 mouse fibroblasts were shown to adhere to the nanofiber scaffold and proliferate *in vitro*, with a 5-fold increase in cell population over a 10-day period. Additionally, cells had begun to migrate through the pores and grow under layers of the fiber network at day 3. It is important to note that while fibers may arrange in a predominately 2-dimensional manner, the developed pores are able to form along any axis, which leads to the formation of a 3-dimensional cellular network. Other work has examined how pore size distribution and pore density can be controlled in order to facilitate cell infiltration. Nam et al. combined electrospinning with salt leaching to create deliberate delaminations, which were connected by electrospun fibers [79]. Within these delaminations cell density was as high as 70% and cells infiltrated as far as 4 mm into the scaffold after 3 weeks of culture. Pham et al. electrospun PCL microfibers and found that as the fiber diameter was increased, the average pore size (with values ranging from 20 to 45 μm) increased while porosity remained constant [80]. In order to combine the nanometer size scale of PCL nanofibers with the larger pores of the PCL microfibers they fabricated layered scaffolds by sequential electrospinning. By varying the electrospinning time they could control the thickness of the nanofiber layers. Using rat marrow stromal cells they demonstrated that increasing the thickness of the nanofiber layer decreased cell infiltration into the scaffold.

As more and more research focuses on developing fibers with smaller diameters in order to maximize surface area, it is important to not overlook the importance of pore size. The pore size of an electrospun scaffold will essentially dictate whether it is viewed as a 2-dimensional mat or a 3-dimensional scaffold by cells. Depending on the application either might be desirable. Additionally, the ability to engineer scaffolds with a desired pore size distribution may allow for the use of nanofibrous scaffolds without limiting cell infiltration, combining the advantages of both micro- and nanofibrous scaffolds.

2.1.4. Surface modification

While the size scale and orientation of nanofibers can be used to influence cell functions such as adhesion, proliferation, and migration, even greater enhancement over the control of cellular function can be achieved by attaching bioactive molecules to the surface of the nanofibrous scaffold. Various groups have examined the effects of attaching different bioactive molecules: the short peptide sequence RGD [40], gelatin [81], perlecan (a natural heparan sulfate proteoglycan) [82], and acrylic acid [43]. Kim et al. examined the effects of grafting the short peptide sequence GRGDY to nanofibrous scaffolds produced via electrospinning of various PLGA/PLGA-b-PEG-NH_2 blends containing different ratios [40]. They observed that the RGD modified

nanofibers demonstrated enhanced attachment, spreading, and proliferation of NIH3T3 fibroblasts as compared to unmodified nanofibers. Thus, the NIH3T3 fibroblasts were forming specific interactions with the RGD peptides, indicating that surface modification of nanofibrous scaffolds with the RGD peptide can be used to further enhance cell interactions with the scaffold. In another study, Ma et al. examined the effects of covalently grafting gelatin to random and aligned PCL nanofibers on endothelial cell (EC) spreading and proliferation [81]. They observed that the presence of gelatin increased both EC spreading and proliferation as compared to unmodified PCL fibers. Thus, surface modification of nanofibrous scaffolds can be used to further enhance the interactions between cells and the scaffold material.

2.1.5. Tissue applications

The process of electrospinning has been found to have great potential in the engineering of a number of tissues including: vasculature [23,52,83–87], bone [48,65,67,88–90], neural [42,49], and tendon/ligament [91,92]. Electrospinning has received great interest in the area of tissue engineered vascular grafts due to the ability to form aligned scaffolds for anisotropic mechanical and biological properties, as well as the ability to prevent smooth muscle cell migration. However, other research has examined how additional properties of electrospun scaffolds can be used to improve upon current vascular grafts. Inoguchi et al. electrospun various tubular scaffolds using poly(L-lactide-*co*-ϵ-caprolactone) for applications as tissue engineered vascular grafts [86]. By varying the wall thickness they were able to create a more compliant scaffold that was responsive to pulsatile flow, thus more accurately mimicking a native artery. In a later experiment, Inoguchi et al. utilized their previously developed compliant poly(L-lactide-*co*-ϵ-caprolactone) electrospun scaffold to examine human umbilical vein endothelial cell (HUVEC) attachment under flow [84]. They demonstrated that gradually increasing the shear stress from 3.2 to 19.6 dyn/cm^2 over a 48-h period as opposed to starting at a high shear stress (8.7 or 19.6 dyn/cm^2) markedly decreased the number of cells detaching from the scaffold. The graded exposure to shear also resulted in highly elongated cells, with their long axis aligned parallel to the direction of flow. Preconditioning endothelial cells prior to implantation is both beneficial and necessary as a confluent endothelium is required in order to prevent thrombosis. Electrospun scaffolds may provide even more beneficial results due to their high fraction of available surface, which aids in cell attachment. Further enhancement of cell attachment and interaction with the scaffold can be achieved through surface modification and inclusion of natural materials. He et al. examined the effects of electrospinning a collagen-blended poly(L-lactic acid)-*co*-poly(ϵ-caprolactone) (P(LLA-CL), 70:30) nanofiber scaffold on human coronary artery endothelial cell (HCAEC) viability and attachment [87]. In an *in vitro* study they demonstrated that incorporation of collagen was able to enhance HCAEC viability, spreading, and attachment, while also preserving the endothelial cell phenotype.

Another tissue for which electrospun nanofiber meshes have emerged as potential scaffolds is bone. Thomas et al. examined the mechanical properties of aligned PCL electrospun nanofiber meshes collected at different rotation speeds (0, 3000, and 6000 RPM) [48]. They observed that the nanofibers became more aligned as the rotation speed increased. They also observed that increasing the rotation speed had a significant effect on the mechanical properties of both the individual nanofibers and the bulk scaffold. The hardness and Young's modulus of individual fibers were found to decrease with increasing rotation speeds. The authors attribute this decrease in mechanical properties to a decrease in fiber crystallinity at higher rotation speeds. However, due to the increased fiber alignment seen at higher rotations speeds, the tensile strength and modulus of the bulk scaffold along the axis of aligned fibers increased with increasing rotation speed. The ultimate tensile strength increased from 2.21 ± 0.23 MPa at a rotation speed of 0 RPM to 9.58 ± 0.71 MPa at a rotation speed of 6000 RPM. Similarly, the tensile modulus increased from 6.12 ± 0.80 MPa at a rotation speed of 0 RPM to 33.20 ± 1.98 MPa at a rotation speed of 6000 RPM. Thus, the authors were able to demonstrate that increasing fiber alignment through the use of high collector rotation speeds actually decreases the mechanical properties of individual fibers, while improving the mechanical properties of the bulk material.

Nie and Wang examined the release of DNA from electrospun scaffolds consisting of a blend of PLGA and Hydroxylapatite (HAp) with various HAp contents (0%, 5%, and 10%) for bone tissue engineering applications [66]. DNA was incorporated into the scaffolds in three ways: (1) naked DNA, (2) adsorption of DNA/chitosan nanoparticles onto scaffolds after fiber fabrication by dripping, or (3) blending DNA/chitosan nanoparticles with the PLGA/HAp solution prior to electrospinning. They observed that higher HAp contents led to faster DNA release for both free and encapsulated DNA. This may be due to the hydrophilic nature of HAp, which caused the DNA/chitosan nanoparticles to bind to HAp particles in the presence of dichloromethane during the emulsion procedure. Not only would this increase encapsulation efficiency, as was noted by the authors, but it would also increase the release rate. As the HAp nanoparticles diffuse out of the PLGA fibers they leave pores through which the DNA/chitosan particles can easily diffuse through. Due to the fact that the DNA/chitosan nanoparticles were associated with the HAp particles during the electrospinning process they will be in close proximity to the pores left behind by the HAp particles. The authors noted that encapsulated DNA/chitosan nanoparticles enhanced transfection efficiency leading to higher cell attachment and viability in an *in vitro* study. Thus, the authors demonstrated that the encapsulation of DNA/chitosan nanoparticles in PLGA/HAp electrospun scaffolds has the potential to augment bone tissue regeneration.

Electrospinning has also been investigated as a polymer processing technique for neural tissue engineering applications. The ability to electrospin nanofiber scaffolds that contain aligned fibers has demonstrated great potential for guiding

neurite outgrowth. Yang et al. examined the performance of both aligned and random PLLA electrospun scaffolds for neural tissue engineering applications [49]. By varying the polymer concentration from 1 to 5% w/w they were also able to produce both nanofibers and microfibers, allowing them to examine the effects of both fiber alignment and fiber diameter on the morphology, differentiation, and neurite outgrowth of neural stem cells (NSCs) *in vitro*. The authors observed that NSCs oriented parallel to the aligned fibers, giving directed neurite outgrowth. However, the NSCs cultured on random PLLA scaffolds did not show a directed orientation. NSCs cultured on aligned nanofibrous scaffolds demonstrated the largest neurite outgrowth with neurites as long as 100 μm after 2 days of culture. Neurite outgrowth was similar on the other scaffolds with average neurite length ranging between 75 and 80 μm. Additionally, the authors observed that the rate of NSC differentiation was faster on nanofibers as compared to microfibers, independent of the fiber alignment. Due to the ability of the aligned scaffolds to orient NSC elongation and neurite outgrowth as well as the ability of nanofibers to increase the rate of differentiation of NSCs, the authors found the aligned nanofibrous scaffold to be ideal for neural tissue engineering applications, demonstrating that not only fiber alignment but also fiber diameter can play an important role in determining the viability of an electrospun scaffold.

One other area where electrospinning has recently received attention as a possible polymer processing technique is for the fabrication of scaffolds to be used in tendon and ligament repair. Due to the relatively high tensile strength of tendon and ligament, the deposition of a collagenous connective tissue matrix is crucial for successful tissue reconstruction. Ouyang et al. examined a knitted PLGA scaffold for applications in tendon regeneration in adult female New Zealand White rabbits with 10 mm gap defects of the Achilles tendon [93]. They observed that the regenerated tendons contained collagen type I and type III fibers as early as 2 weeks postimplantation. Additionally, at 12 weeks postimplantation both the tensile stiffness and modulus of the regenerated tendon were more than 50% that of normal tendon, with even better results achieved for scaffolds seeded with bone marrow stromal cells. Despite these promising results, knitted scaffolds often require gel systems for successful cell seeding, which may not be suitable for certain situations where the gel system is more prone to dissociate from the knit scaffold. Thus, Sahoo et al. electrospun PLGA nanofibers onto a knitted PLGA scaffold in order to provide a large area for cell attachment; thereby, removing the need for a gel system for cell seeding [91]. The authors then examined porcine bone marrow stromal cell attachment, proliferation, and extracellular matrix synthesis on the electrospun/knit composite scaffold as compared to a knit PLGA scaffold in which cells were immobilized using a fibrin gel. They found that cell proliferation and cellular activity were both increased in the electrospun/knit composite scaffold, while the cell attachment was comparable between the two scaffolds. Additionally, Lee et al. found that human ligament fibroblasts synthesize significantly larger amounts of collagen when they are seeded on aligned nanofibers as compared to randomly oriented nanofibers [92]. Thus, electrospun nanofibrous scaffolds can be used not only to improve cell attachment but also to increase cellular activity such as extracellular matrix generation in tissue engineering scaffolds for tendon/ligament repair.

2.2. Drug delivery

Electrospinning affords great flexibility in selecting materials for drug delivery applications. Either biodegradable or non-degradable materials can be used to control whether drug release occurs via diffusion alone or diffusion and scaffold degradation. Additionally, due to the flexibility in material selection a number of drugs can be delivered including: antibiotics, anticancer drugs, proteins, and DNA. Using the various electrospinning techniques a number of different drug loading methods can also be utilized: coatings, embedded drug, and encapsulated drug (coaxial and emulsion electrospinning). These techniques can be used to give finer control over drug release kinetics.

2.2.1. Materials

When selecting a material to use in a drug delivery device a number of requirements must be met. As with materials used in tissue engineering applications, materials that undergo biodegradation are generally more popular due to the fact that they eliminate the need for explantation. However, biodegradable materials add an extra level of complexity to drug delivery devices as compared to non-degradable materials, which tend to release drug primarily by diffusion. Generally it is desirable to design a drug delivery device that gives controlled release of the desired agent; however, this may be difficult if the material begins degrading as the drug is being released. In a biodegradable system the drug may be released by diffusion as well as degradation of the material, which in some cases can lead to dose dumping resulting in local drug concentrations reaching toxic levels. Thus, special care must be taken to tailor both the release rate and the degradation rate if a degradable material is to be used.

Chew et al. examined the release of β-nerve growth factor (NGF) stabilized in BSA from a copolymer consisting of ϵ-caprolactone and ethyl ethylene phosphate (PCLEEP) [50]. Due to its relatively hydrophobic backbone, PCLEEP has a slow degradation rate demonstrating a mass loss of approximately 7% over a 3-month period. Using this system, Chew et al. observed a sustained release of NGF over a period of 3 months. Due to the relatively small amount of mass loss over this period they inferred that NGF release was occurring primarily via diffusion, demonstrating that a biodegradable system can be used to obtain a desirable release profile while still eliminating the need for a second surgery for implant removal. Kenawy et al. examined the release of tetracycline hydrochloride from electrospun mats composed of PLA, poly(ethylene-*co*-vinyl acetate) (PEVA), and a 50:50 blend of the two [94]. The electrospun mats were prepared by dissolving the polymer (14% w/v) and tetracycline hydrochloride (5 or 25 wt%) in a chloroform/methanol solution, thus

producing polymer fibers containing embedded drug. The authors found that both polymer composition and drug loading affected the rate of drug release with PEVA demonstrating quicker release than either the 50:50 PEVA/PLA blend or PLA. Additionally, the authors compared the release profile obtained from electrospun mats to those obtained from corresponding cast films. Due to their larger surface areas, electrospun mats tended to give greater release of drug than did the corresponding films. Additionally, the electrospun PEVA and 50:50 PEVA/PLA mats gave a relatively smooth release over a period of 5 days, while eliminating the initial burst seen with the films.

2.2.2. Drugs/drug loading

Recent work has examined the possibility of using electrospun matrices as constructs for giving controlled release of a number of drugs including antibiotics [95–97] and anticancer drugs [98,99]; as well as proteins [31,33,50,66] and DNA [66,90,100] for applications in tissue engineering (Table 2). Following an invasive surgery in a region such as the abdominal wall, it is common to deliver antibiotics either systemically or locally in order to prevent infection at the surgery site. While infection is a potential complication with any surgery, one of the main complications encountered at the abdominal wall postsurgery is the formation of fibrotic bands linking separate surfaces in the peritoneal cavity, known as abdominal adhesion. Additionally, previous work has indicated that the formation of abdominal adhesions can be increased by certain bacteria [95]. Thus, while the most promising technique for preventing abdominal adhesion postsurgery remains the use of a physical barrier to separate the injured site from the adjacent tissues, incorporation of antibiotics has also shown promise. A scaffold that is capable of providing barrier function along with controlled delivery of a substantial amount of antibiotic could potentially decrease the frequency and severity of abdominal adhesion formation postsurgery.

Due to the ability to fabricate scaffolds containing pores on the nanometer size scale, which can either limit or eliminate cell migration; as well as scaffolds with inherently high surface area, which allows for high drug loadings and the ability to overcome mass transfer limitations associated with other polymeric systems, electrospun matrices are able to meet both requirements of barrier function and drug delivery necessary to prevent abdominal adhesion. Bolgen et al. examined the potential of PCL electrospun mats loaded with a commercial antibiotic (Biteral®) for preventing abdominal adhesion following surgery in a rat model [95]. PCL (13% w/v) in chloroform/DMF (30:70) was initially electrospun to form a nonwoven fibrous mat, which was then covered with a solution of Biteral®. Thus, drug loading was achieved by absorption of the Biteral® solution into the electrospun mat and drug was only located at the surfaces of the electrospun fibers. *In vitro* release studies demonstrated that nearly 80% of the drug was released after the first 3 h, with complete release occurring after almost 18 h. The authors suggest that this rapid burst release of drug is advantageous as most infections occur within a few hours after surgery. Adhesion was then examined *in vivo* using a rat model with defects in the abdominal wall in the peritoneum. A control containing no scaffold was examined along with electrospun PCL mats with or without antibiotic. The authors found that both the extent and tenacity of abdominal adhesions was reduced using the antibiotic containing electrospun PCL mat as compared to the control and the unloaded PCL mat. Additionally, the antibiotic containing electrospun PCL mat seemed to improve and accelerate the healing process as compared to the control and the unloaded PCL mat. However, the authors noted that the electrospun mats degraded much slower than the rate of the healing process, indicating that the fiber diameter must be reduced and lower molecular weight polymer must be used in order to tailor the degradation rate to the healing rate *in vivo*. Thus, antibiotic loaded electrospun scaffolds have potential applications in reducing abdominal adhesion postsurgery.

Kim et al. examined the controlled release of a hydrophilic antibiotic (Mefoxin®) from electrospun PLGA and PLGA/PEG-b-PLA/PLA (80:15:5 by wt%) mats, but used a different method of drug loading than that found in Bolgen et al. [97]. Rather than absorbing the antibiotic onto the scaffold after electrospinning, Kim et al. dissolved both the polymer and the antibiotic in DMF prior to electrospinning, giving antibiotic embedded within the electrospun fibers. The authors observed that the drug loading affected the morphology of the electrospun fibers, with solutions containing no drug giving a bead-and-string morphology and solutions containing 5 wt% drug giving a completely fibrous structure. Additionally, the average fiber diameter decreased from 360 ± 220 nm (without drug) to 260 ± 90 nm (with 5 wt% of drug). The authors attribute this change in morphology and fiber diameter to the increased conductivity of the solutions containing drug. The authors also verified that the structure of the drug was unchanged by the electrospinning process using both UV–vis and ^{1}H NMR analysis, demonstrating that the antibiotic retained its bioactivity. An *in vitro* drug release study was conducted and demonstrated that the PLGA/PEG-b-PLA/PLA blend gave a more sustained release than did the PLGA mat. The authors suggest that due to the high ionic strength of the drug and the minimal physical interactions between the polymer and the drug in the PLGA system, the drug is primarily located at the surface of the fibers. However, incorporating the amphiphilic PEG-b-PLA block copolymer allows some of the hydrophilic antibiotic to be embedded in the polymer nanofibers. Additionally, electrospun PLGA and PLGA/PEG-b-PLA/PLA mats containing 5 wt% antibiotic both demonstrated greater than 90% inhibition of *Staphylococcus aureus* growth. Thus, the authors demonstrated that antibiotic loaded electrospun mats can be used to effectively reduce infection; however, careful attention must be paid to polymer composition as it can affect drug loading and consequently the drug release profile.

One of the largest areas of research within the drug delivery field is the targeted and controlled delivery of anticancer drugs. Electrospun mats have the ability to overcome drug loading limitations seen with other drug delivery devices, such as micelles and liposomes, currently used for targeting

Table 2
Electrospun polymers for drug delivery and tissue engineering applications

No.	Polymer	Solvent	Fiber diameter	Nozzle configuration	Application (cell type/drug)	Ref.
General tissue engineering (T.E.)						
1	Poly(ϵ-caprolactone)	(a) Chloroform and methanol (b) Chloroform and DMF	2–10 μm ~600 nm	Single nozzle	General T.E. (rat marrow stromal cells)	[80]
2	(a) Poly(ϵ-caprolactone) (core) (b) Zein (shell)	(a) Chloroform and DMF (b) DMF	500–900 nm	Coaxial	General T.E. (none used)	[27]
3	(a) Poly(ϵ-caprolactone) (core) (b) Collagen (shell)	(a) 2,2,2-trifluoroethanol (b) 2,2,2-trifluoroethanol	~513 nm	Coaxial	General T.E. (human dermal fibroblasts)	[32]
4	Poly(D,L-lactic-*co*-glycolic acid) and PLGA-b-PEG-NH_2	DMF and THF	449–1312 nm	Single nozzle	General T.E. (NIH3T3 fibroblasts)	[40]
5	Poly(D,L-lactide-*co*-glycolide)	DMF and THF	500–800 nm	Single nozzle	General T.E. (human mesenchymal stem cells and BALB/c C7 mouse fibroblasts)	[78]
6	Poly(ethylene glycol-*co*-lactide)	DMF and acetone	1.25–4.25 μm	Single nozzle	General T.E. (none used)	[41]
7	Poly(ethylene-*co*-vinyl alcohol)	2-propanol and water	0.2–8.0 μm	Single nozzle	General T.E. (human aortic smooth muscle cells and human dermal fibroblasts)	[55]
8	Collagen	HFP	180–250 nm	Single nozzle	General T.E. (rabbit conjunctiva fibroblasts)	[56]
9	Collagen	HFP	100–730 nm	Single nozzle	General T.E. (aortic smooth muscle cells)	[57]
10	(a) Collagen (b) Gelatin	(a) HFP and acetic acid (b) HFP	3–6 μm 2–6 μm	Single nozzle	General T.E. (human osteosarcoma cells)	[82]
11	Gelatin	2,2,2-trifluoroethanol	0.29–9.10 μm	Single nozzle	General T.E. (none used)	[60]
12	Fibrinogen	HFP and 10X minimal essential medium	0.12–0.61 μm	Single nozzle	General T.E. (neonatal rat cardiac fibroblasts)	[61]
13	Poly(glycolic acid) and chitin	HFP	130–380 nm	Single nozzle	General T.E. (normal human epidermal fibroblasts)	[70]
14	Collagen and Poly(ethylene oxide)	10 mM HCl (pH 2.0)	100–150 nm	Single nozzle	General T.E. (none used)	[72]
15	Poly(DTE carbonate)	DCM	1.9–5.8 μm	Single nozzle	General T.E. (NIH3T3 (mouse embryo fibroblasts), MCF-7 (human mammary carcinoma), PC-12 (rat adrenal pheochromocytoma) and KB (KB/HeLa; human cervical carcinoma))	[16]
Vascular T.E.						
1	Poly(ϵ-caprolactone)	Chloroform and DMF	0.2–1 μm	Single nozzle	Vascular T.E. (human coronary artery endothelial cells)	[81]
2	Poly(D,L-lactide-*co*-glycolide), collagen, and elastin	HFP	720 ± 350 nm	Single nozzle	Vascular T.E. (bovine endothelial and smooth muscle cells)	[23]
3	Poly(L-lactide-*co*-ϵ-caprolactone)	Acetone	200–800 nm	Single nozzle	Vascular T.E. (human coronary artery smooth muscle cells)	[52]
4	Poly(L-lactide-*co*-ϵ-caprolactone)	HFP	799–820 nm	Single nozzle	Vascular T.E. (human umbilical vein endothelial cells (HUVECs))	[84]
5	Poly(L-lactide-*co*-ϵ-caprolactone)	HFP	700–800 nm	Single nozzle	Vascular T.E. (none used)	[86]
6	Poly(L-lactide-*co*-ϵ-caprolactone) and collagen	HFP	100–300 nm	Single nozzle	Vascular T.E. (human coronary artery endothelial cells (HCAECs))	[87]
7	Poly(propylene carbonate)	Chloroform	~5 μm	Single nozzle	Vascular T.E. (rat bone marrow mesenchymal stem cells)	[85]
Neural T.E.						
1	(a) Poly(ϵ-caprolactone) (b) Poly(ϵ-caprolactone) and collagen	(a) Chloroform and methanol (b) HFP	559 ± 300 nm 541 ± 164 nm	Single nozzle	Neural T.E. (DRG explants, dissociated DRG, Schwann cells, olfactory ensheathing cells, and fibroblasts)	[42]
2	Poly(L-lactic acid)	DMF and DCM	300–3500 nm	Single nozzle	Neural T.E. (mouse neural stem cells)	[49]
Bone T.E.						
1	Poly(L-lactic acid) and hydroxylapatite	DCM and 1,4-dioxane	~313 nm	Single nozzle	Bone T.E. (MG-63 osteoblasts)	[64]
Skin T.E.						
1	Chitin	HFP	0.163–8.77 μm	Single nozzle	Skin T.E. (normal human oral keratinocytes, normal human epidermal keratinocytes, and normal human gingival fibroblasts)	[62]
Drug delivery systems (D.D.S.)						
1	(a) Poly(ϵ-caprolactone) (shell) (b) Poly(ethylene glycol) (core)	(a) 2,2,2-trifluoroethanol (b) Water	270–380 nm	Coaxial	D.D.S. (fitcBSA)	[28]

(*continued on next page*)

Table 2 (*continued*)

No.	Polymer	Solvent	Fiber diameter	Nozzle configuration	Application (cell type/drug)	Ref.
2	(a) Poly(ϵ-caprolactone) and poly(ethylene glycol) (shell) (b) Dextran (core)	(a) Chloroform and DMF (b) Water	1.1–5.7 μm	Coaxial	D.D.S. (BSA)	[31]
3	(a) Poly(ϵ-caprolactone) (shell) (b) Poly(ethylene glycol) (core)	(a) Chloroform and DMF (b) Water	545–774 nm	Coaxial	D.D.S. (BSA and lysozyme)	[33]
4	Poly(ϵ-caprolactone-*co*-ethyl ethylene phosphate)	DCM and PBS	0.46–5.01 μm	Single nozzle	D.D.S. (β-nerve growth factor and BSA)	[50]
5	Poly(D,L-lactic-*co*-glycolic acid), PEG-b-PLA, and PLA	DMF	260–360 nm	Single nozzle	D.D.S. (Mefoxin®, cefoxitin sodium)	[98]
6	Poly(D,L-lactic-*co*-glycolic acid)	DCM	0.03–10 μm	Single nozzle	D.D.S. (Paclitaxel)	[100]
7	Poly(L-lactide-*co*-glycolide) and PEG-PLLA	Chloroform	690–1350 nm	Single nozzle	D.D.S. (BCNU)	[99]

Abbreviations: T.E.: tissue engineering; D.D.S.: drug delivery systems; DMF: *N*,*N*-dimethylformamide; THF: tetrahydrofuran; DCM: dichloromethane; HFP: 1,1,1,3,3,3-hexafluoro-2-propanol; PBS: phosphate buffered saline; HCl: hydrochloric acid; BSA: bovine serum albumin; and DRG: dorsal root ganglia.

tumors. Xu et al. examined the incorporation of the anticancer drug BCNU into electrospun PEG-PLLA mats [98]. Both the polymer and the BCNU were dissolved in chloroform and electrospun, giving BCNU embedded in the PEG-PLLA fibers. The authors used an environmental scanning electron microscope with an EDS accessory to demonstrate that uniform fibers with relatively smooth surfaces were obtained as well as a uniform drug distribution. The average fiber diameters depended on drug loading with values ranging from 690 to 1350 nm for drug loadings of 5 and 30 wt%, respectively. Both the release rate and the initial burst release increased with increasing BCNU loading. The effect of BCNU release from electrospun PEG-PLLA mats on the growth of rat Glioma C6 cells was also examined. While unloaded PEG-PLLA fibers did not have any affect on cell growth, BCNU loaded PEG-PLLA mats exhibited anticancer activity over a period of 72 h, while free BCNU began to lose its anticancer activity after 48 h. Thus, by embedding the drug in the polymer fibers the authors were able to protect it from degradation and preserve its anticancer activity. Additionally, the authors were able to effectively control the release rate of BCNU from the electrospun mats by altering the drug loading.

Xie and Wang also examined the treatment of C6 gliomas; however, they used an electrospun PLGA mat to encapsulate the anticancer drug Paclitaxel [99]. By varying the processing parameters they were able to produce fibers with average diameters ranging from the tens of nanometers to 10 μm. Fibers with diameters around 30 nm were obtained after adding the organic salt tetrabutylammonium tetraphenylborate (TATPB), which increased the conductivity of the solution. SEM images indicated that electrospun fibers had porous surfaces with pore size depending on the solution flow rate. The authors also determined that encapsulation efficiency of the Paclitaxel loaded electrospun PLGA mats was more than 90%. An *in vitro* drug release study demonstrated controlled release from both PLGA nano- and microfibers over a period of 61 days. Nanofibers had a faster release rate, releasing approximately 80% of the drug over the 61-day release period as compared to approximately 60% for the microfibers. Additionally, the release rates for both systems (nano and micro) were nearly linear with respect to the square root of time, indicative of first order kinetics. An *in vitro* cytotoxicity study demonstrated that depending on the drug loading, up to 70% of C6 Glioma cells could be killed after 72 h.

While drug delivery is often associated with the delivery of therapeutic agents for the treatment of some disease state such as cancer, it can also apply to the delivery of bioactive agents such as proteins and DNA for tissue engineering applications. While the size scale and topography of electrospun nanofibers can help aid in cell attachment and proliferation due to their close approximation to the extracellular matrix, the ability to control the spatial and temporal delivery of bioactive agents can further augment the scaffolds ability to promote cell attachment, proliferation, and differentiation. Jiang et al. used a coaxial electrospinning setup to fabricate biodegradable core-shell fibers with PCL as the shell and BSA containing dextran as the core [31]. Both BSA loading and its release rate could be controlled by varying the feed rate of the inner solution, with higher feed rates giving higher BSA loading and accelerated release. Addition of PEG to the shell was used to further control the release rate, and was shown to increase release of BSA. By varying the inner solution feed rate as well as the PEG content of the shell the authors were able to vary the release period from 1 week to approximately 1 month. Liang et al. examined the incorporation of DNA into electrospun PLGA scaffolds [100]. Plasmid DNA was condensed in a poor solvent mixture, and was then encapsulated in micelles composed of a triblock copolymer (PLA–PEG–PLA) giving encapsulated DNA nanoparticles. The micelles were then dissolved in a solution of DMF with PLGA and electrospun, resulting in the formation of PLGA fibers containing encapsulated DNA nanoparticles. The DNA was encapsulated in the PLA–PEG–PLA triblock copolymer in order to protect it from degradation during electrospinning with the PLGA copolymer. An *in vitro* release study demonstrated that approximately 20% of the encapsulated DNA was released after a period of 7 days. Additionally, the authors also examined the encapsulation of DNA in PLGA fibers without first forming protective micelles using the PLA–PEG–PLA triblock copolymer. MC3T3 cells demonstrated no transfection when the PLGA/DNA system

(without the PLA–PEG–PLA triblock copolymer) was used. However, the PLGA/PLA–PEG–PLA/DNA system did demonstrate some limited transfection. The authors attribute the lack of transfection in the system without the PLA–PEG–PLA triblock copolymer to degradation of the DNA during the electrospinning process. This paper demonstrates the importance of protecting biological agents that are incorporated into electrospun scaffolds. Special care must be taken to ensure that the agents will retain their bioactivity.

3. Conclusions

In recent years electrospinning has gained widespread interest as a potential polymer processing technique for applications in drug delivery and tissue engineering. This renewed interest can be attributed to electrospinning's relative ease of use, adaptability, and the ability to fabricate fibers with diameters on the nanometer size scale. While much has been learned about the electrospinning process over its long history, researchers are still gaining new insights and developing new ways of utilizing this technique for tissue engineering and drug delivery applications. The development of new nozzle configurations has led to the development of fibers with a core-shell morphology, which have shown promise in providing sustained drug release as well as in mitigating the initial burst release seen with polymer/drug blends. The development of new collectors has demonstrated the importance in choosing the correct collector properties in order to obtain the desired scaffold properties (e.g. pore size and fiber density). Additionally, different collectors can be used to control not only the scaffold geometry but also the fiber alignment, which can be used to control the mechanical properties as well as the biological response to the scaffold. Research has shown that surface modification of electrospun fibers can be used to further enhance the scaffold's interaction with cells in tissue engineering applications. The ability to electrospin synthetic (biodegradable or non-degradable), natural, and hybrid materials allows for precise tailoring of the scaffold properties to the desired application, and new materials are constantly being electrospun. While electrospinning has emerged as a viable polymer processing technique for applications in drug delivery and tissue engineering, its true potential has yet to be realized. In the future it is important that research focuses on gaining a better fundamental understanding of the electrospinning process, but even more importantly on how this technique can be used as a tool in developing new systems for drug delivery and tissue engineering. In this review the most recent and state of the artwork in electrospinning for applications in tissue engineering and drug delivery have been briefly discussed with the hope that this information will help researchers plan and conduct future research in the field of electrospinning.

Acknowledgements

We would like to thank Nick Wang of Case Western Reserve University for his help in preparing this manuscript. This work was funded, in part, through a grant from the Ohio Department of Development Third Frontier Program, Biotechnology Research and Training Transfer Grant Number 05-065 to the Clinical Tissue Engineering Center; and also in part by an Innovative Incentive Fellowship from the Ohio Board of Regents.

References

[1] Formhals A, inventor. Process and apparatus for preparing artificial threads. US Patent No. 1,975,504; 1934.
[2] Formhals A, inventor. Method and apparatus for spinning. US Patent No. 2,169,962; 1939.
[3] Formhals A, inventor. Artificial thread and method of producing same. US Patent No. 2,187,306; 1940.
[4] Taylor G. Electrically driven jets. Proc Natl Acad Sci London 1969;A313(1515):453–75.
[5] Baumgarten P. Electrostatic spinning of acrylic microfibers. J Colloid Interface Sci 1971;36(1):71–9.
[6] Larrondo L, Manley RSJ. Electrostatic fiber spinning from polymer melts. 1. Experimental-observations on fiber formation and properties. J Polym Sci B Polym Phys 1981;19(6):909–20.
[7] Larrondo L, Manley RSJ. Electrostatic fiber spinning from polymer melts. 2. Examination of the flow field in an electrically driven jet. J Polym Sci B Polym Phys 1981;19(6):921–32.
[8] Annis D, Bornat A, Edwards RO, Higham A, Loveday B, Wilson J. An elastomeric vascular prosthesis. Trans Am Soc Artif Intern Organs 1978;24:209–14.
[9] Fisher AC, De Cossart L, How TV, Annis D. Long term in-vivo performance of an electrostatically-spun small bore arterial prosthesis: the contribution of mechanical compliance and anti-platelet therapy. Life Support Syst 1985;1(3 Suppl):462–5.
[10] Yarin AL, Koombhongse S, Reneker DH. Bending instability in electrospinning of nanofibers. J Appl Phys 2001 Mar 1;89(5):3018–26.
[11] Doshi J, Reneker DH. Electrospinning process and applications of electrospun fibers. J Electrostatics 1995 Aug;35(2–3):151–60.
[12] Warner S, Buer A, Grimler M, Ugbolue S, Rutledge G, Shin M. Nano fibers. Natl Text Cent Annu Rep 1998:83.
[13] Shin YM, Hohman MM, Brenner MP, Rutledge GC. Electrospinning: a whipping fluid jet generates submicron polymer fibers. Appl Phys Lett 2001 Feb 19;78(8):1149–51.
[14] Liu HQ, Hsieh YL. Ultrafine fibrous cellulose membranes from electrospinning of cellulose acetate. J Polym Sci B Polym Phys 2002 Sep 15;40(18):2119–29.
[15] Deitzel JM, Kleinmeyer J, Harris D, Tan NCB. The effect of processing variables on the morphology of electrospun nanofibers and textiles. Polymer 2001 Jan;42(1):261–72.
[16] Meechaisue C, Dubin R, Supaphol P, Hoven VP, Kohn J. Electrospun mat of tyrosine-derived polycarbonate fibers for potential use as tissue scaffolding material. J Biomater Sci Polym Ed 2006;17(9):1039–56.
[17] Megelski S, Stephens JS, Chase DB, Rabolt JF. Micro- and nanostructured surface morphology on electrospun polymer fibers. Macromolecules 2002 Oct 22;35(22):8456–66.
[18] Jaeger R, Bergshoef MM, Batlle CMI, Schonherr H, Vancso GJ. Electrospinning of ultra-thin polymer fibers. Macromol Symp 1998 Feb;127:141–50.
[19] Hayati I, Bailey AI, Tadros TF. Investigations into the mechanisms of electrohydrodynamic spraying of liquids. 1. Effect of electric-field and the environment on pendant drops and factors affecting the formation of stable jets and atomization. J Colloid Interface Sci 1987 May;117(1):205–21.
[20] Zhang CX, Yuan XY, Wu LL, Han Y, Sheng J. Study on morphology of electrospun poly(vinyl alcohol) mats. Eur Poly J 2005 Mar;41(3):423–32.
[21] Jiang H, Fang D, Hsiao BS, Chu B, Chen W. Optimization and characterization of dextran membranes prepared by electrospinning. Biomacromolecules 2004 Mar–Apr;5(2):326–33.

[22] Tan EP, Ng SY, Lim CT. Tensile testing of a single ultrafine polymeric fiber. Biomaterials 2005 May;26(13):1453–6.
[23] Stitzel J, Liu J, Lee SJ, Komura M, Berry J, Soker S, et al. Controlled fabrication of a biological vascular substitute. Biomaterials 2006 Mar;27(7):1088–94.
[24] Qi H, Hu P, Xu J, Wang A. Encapsulation of drug reservoirs in fibers by emulsion electrospinning: morphology characterization and preliminary release assessment. Biomacromolecules 2006 Aug;7(8):2327–30.
[25] Gupta P, Wilkes GL. Some investigations on the fiber formation by utilizing a side-by-side bicomponent electrospinning approach. Polymer 2003 Sep;44(20):6353–9.
[26] Zhao P, Jiang H, Pan H, Zhu K, Chen W. Biodegradable fibrous scaffolds composed of gelatin coated poly(epsilon-caprolactone) prepared by coaxial electrospinning. J Biomed Mater Res A 2007 Nov;83(2):372–82.
[27] Jiang H, Zhao P, Zhu K. Fabrication and characterization of zein-based nanofibrous scaffolds by an electrospinning method. Macromol Biosci 2007 Apr 10;7(4):517–25.
[28] Zhang YZ, Wang X, Feng Y, Li J, Lim CT, Ramakrishna S. Coaxial electrospinning of (fluorescein isothiocyanate-conjugated bovine serum albumin)-encapsulated poly(epsilon-caprolactone) nanofibers for sustained release. Biomacromolecules 2006 Apr;7(4):1049–57.
[29] Townsend-Nicholson A, Jayasinghe SN. Cell electrospinning: a unique biotechnique for encapsulating living organisms for generating active biological microthreads/scaffolds. Biomacromolecules 2006 Dec;7(12): 3364–9.
[30] McCann JT, Marquez M, Xia Y. Melt coaxial electrospinning: a versatile method for the encapsulation of solid materials and fabrication of phase change nanofibers. Nano Lett 2006 Dec;6(12):2868–72.
[31] Jiang H, Hu Y, Zhao P, Li Y, Zhu K. Modulation of protein release from biodegradable core-shell structured fibers prepared by coaxial electrospinning. J Biomed Mater Res B Appl Biomater 2006 Oct;79(1):50–7.
[32] Zhang YZ, Venugopal J, Huang ZM, Lim CT, Ramakrishna S. Characterization of the surface biocompatibility of the electrospun PCL-collagen nanofibers using fibroblasts. Biomacromolecules 2005 Sep–Oct;6(5):2583–9.
[33] Jiang H, Hu Y, Li Y, Zhao P, Zhu K, Chen W. A facile technique to prepare biodegradable coaxial electrospun nanofibers for controlled release of bioactive agents. J Control Release 2005 Nov 28;108(2–3):237–43.
[34] Dalton PD, Lleixa Calvet J, Mourran A, Klee D, Moller M. Melt electrospinning of poly-(ethylene glycol-block-epsilon-caprolactone). Biotechnol J 2006 Sep;1(9):998–1006.
[35] Flemming RG, Murphy CJ, Abrams GA, Goodman SL, Nealey PF. Effects of synthetic micro- and nano-structured surfaces on cell behavior. Biomaterials 1999 Mar;20(6):573–88.
[36] von Recum A, Shannon C, Cannon C, Long K, van Kooten T, Meyle J. Surface roughness, porosity, and texture as modifiers of cellular adhesion. Tissue Eng 1996;2(4):241–53.
[37] Green AM, Jansen JA, van der Waerden JP, von Recum AF. Fibroblast response to microtextured silicone surfaces: texture orientation into or out of the surface. J Biomed Mater Res 1994 May;28(5): 647–53.
[38] Sharma B, Elisseeff JH. Engineering structurally organized cartilage and bone tissues. Ann Biomed Eng 2004 Jan;32(1):148–59.
[39] Liu X, Ma PX. Polymeric scaffolds for bone tissue engineering. Ann Biomed Eng 2004 Mar;32(3):477–86.
[40] Kim TG, Park TG. Biomimicking extracellular matrix: cell adhesive RGD peptide modified electrospun poly(D,L-lactic-*co*-glycolic acid) nanofiber mesh. Tissue Eng 2006 Feb;12(2):221–33.
[41] Yang DJ, Zhang LF, Xu L, Xiong CD, Ding J, Wang YZ. Fabrication and characterization of hydrophilic electrospun membranes made from the block copolymer of poly(ethylene glycol-*co*-lactide). J Biomed Mater Res A 2007 Sep 1;82(3):680–8.
[42] Schnell E, Klinkhammer K, Balzer S, Brook G, Klee D, Dalton P, et al. Guidance of glial cell migration and axonal growth on electrospun nanofibers of poly-epsilon-caprolactone and a collagen/poly-epsilon-caprolactone blend. Biomaterials 2007 Jul;28(19): 3012–25.
[43] Park K, Ju YM, Son JS, Ahn KD, Han DK. Surface modification of biodegradable electrospun nanofiber scaffolds and their interaction with fibroblasts. J Biomater Sci Polym Ed 2007;18(4):369–82.
[44] Li WJ, Mauck RL, Cooper JA, Yuan X, Tuan RS. Engineering controllable anisotropy in electrospun biodegradable nanofibrous scaffolds for musculoskeletal tissue engineering. J Biomech 2007;40(8): 1686–93.
[45] Henry JA, Simonet M, Pandit A, Neuenschwander P. Characterization of a slowly degrading biodegradable polyester-urethane for tissue engineering scaffolds. J Biomed Mater Res A 2007 Sep 1;82(3): 669–79.
[46] Duan B, Wu L, Li X, Yuan X, Li X, Zhang Y, et al. Degradation of electrospun PLGA-chitosan/PVA membranes and their cytocompatibility *in vitro*. J Biomater Sci Polym Ed 2007;18(1):95–115.
[47] Ashammakhi N, Ndreu A, Piras AM, Nikkola L, Sindelar T, Ylikauppila H, et al. Biodegradable nanomats produced by electrospinning: expanding multifunctionality and potential for tissue engineering. J Nanosci Nanotechnol 2007 Mar;7(3):862–82.
[48] Thomas V, Jose MV, Chowdhury S, Sullivan JF, Dean DR, Vohra YK. Mechano-morphological studies of aligned nanofibrous scaffolds of polycaprolactone fabricated by electrospinning. J Biomater Sci Polym Ed 2006;17(9):969–84.
[49] Yang F, Murugan R, Wang S, Ramakrishna S. Electrospinning of nano/microscale poly(L-lactic acid) aligned fibers and their potential in neural tissue engineering. Biomaterials 2005 May;26(15):2603–10.
[50] Chew SY, Wen J, Yim EK, Leong KW. Sustained release of proteins from electrospun biodegradable fibers. Biomacromolecules 2005 Jul–Aug;6(4):2017–24.
[51] Zong X, Li S, Chen E, Garlick B, Kim KS, Fang D, et al. Prevention of postsurgery-induced abdominal adhesions by electrospun bioabsorbable nanofibrous poly(lactide-*co*-glycolide)-based membranes. Ann Surg 2004 Nov;240(5):910–5.
[52] Xu CY, Inai R, Kotaki M, Ramakrishna S. Aligned biodegradable nanofibrous structure: a potential scaffold for blood vessel engineering. Biomaterials 2004 Feb;25(5):877–86.
[53] Kim K, Yu M, Zong X, Chiu J, Fang D, Seo YS, et al. Control of degradation rate and hydrophilicity in electrospun non-woven poly(D,L-lactide) nanofiber scaffolds for biomedical applications. Biomaterials 2003 Dec;24(27):4977–85.
[54] Li WJ, Laurencin CT, Caterson EJ, Tuan RS, Ko FK. Electrospun nanofibrous structure: a novel scaffold for tissue engineering. J Biomed Mater Res 2002 Jun 15;60(4):613–21.
[55] Chuangchote S, Supaphol P. Fabrication of aligned poly (vinyl alcohol) nanofibers by electrospinning. J Nanosci Nanotechnol 2006 Jan;6(1): 125–9.
[56] Kenawy el R, Layman JM, Watkins JR, Bowlin GL, Matthews JA, Simpson DG, et al. Electrospinning of poly(ethylene-*co*-vinyl alcohol) fibers. Biomaterials 2003 Mar;24(6):907–13.
[57] Zhong S, Teo WE, Zhu X, Beuerman RW, Ramakrishna S, Yung LY. An aligned nanofibrous collagen scaffold by electrospinning and its effects on *in vitro* fibroblast culture. J Biomed Mater Res A 2006 Dec 1;79(3):456–63.
[58] Matthews JA, Wnek GE, Simpson DG, Bowlin GL. Electrospinning of collagen nanofibers. Biomacromolecules 2002 Mar–Apr;3(2):232–8.
[59] Matsuda A, Kagata G, Kino R, Tanaka J. Preparation of chitosan nanofiber tube by electrospinning. J Nanosci Nanotechnol 2007 Mar;7(3):852–5.
[60] Song JH, Kim HE, Kim HW. Production of electrospun gelatin nanofiber by water-based co-solvent approach. J Mater Sci Mater Med 2007 Jun 19.
[61] Ayres C, Bowlin GL, Henderson SC, Taylor L, Shultz J, Alexander J, et al. Modulation of anisotropy in electrospun tissue-engineering scaffolds: analysis of fiber alignment by the fast Fourier transform. Biomaterials 2006 Nov;27(32):5524–34.
[62] McManus MC, Boland ED, Simpson DG, Barnes CP, Bowlin GL. Electrospun fibrinogen: feasibility as a tissue engineering scaffold in a rat cell culture model. J Biomed Mater Res A 2007 May;81(2): 299–309.

[63] Noh HK, Lee SW, Kim JM, Oh JE, Kim KH, Chung CP, et al. Electrospinning of chitin nanofibers: degradation behavior and cellular response to normal human keratinocytes and fibroblasts. Biomaterials 2006 Jul;27(21):3934–44.
[64] Ji Y, Ghosh K, Shu XZ, Li B, Sokolov JC, Prestwich GD, et al. Electrospun three-dimensional hyaluronic acid nanofibrous scaffolds. Biomaterials 2006 Jul;27(20):3782–92.
[65] Sui G, Yang X, Mei F, Hu X, Chen G, Deng X, et al. Poly-L-lactic acid/hydroxyapatite hybrid membrane for bone tissue regeneration. J Biomed Mater Res A 2007 Aug;82(2):445–54.
[66] Nie H, Wang CH. Fabrication and characterization of PLGA/HAp composite scaffolds for delivery of BMP-2 plasmid DNA. J Control Release 2007 Jul 16;120(1–2):111–21.
[67] Mohammadi Y, Soleimani M, Fallahi-Sichani M, Gazme A, Haddadi-Asl V, Arefian E, et al. Nanofibrous poly(epsilon-caprolactone)/poly(vinyl alcohol)/chitosan hybrid scaffolds for bone tissue engineering using mesenchymal stem cells. Int J Artif Organs 2007 Mar;30(3):204–11.
[68] Meng W, Kim SY, Yuan J, Kim JC, Kwon OH, Kawazoe N, et al. Electrospun PHBV/collagen composite nanofibrous scaffolds for tissue engineering. J Biomater Sci Polym Ed 2007;18(1):81–94.
[69] Duan B, Wu L, Yuan X, Hu Z, Li X, Zhang Y, et al. Hybrid nanofibrous membranes of PLGA/chitosan fabricated via an electrospinning array. J Biomed Mater Res A 2007 Dec 1;83(3):868–78.
[70] Peesan M, Rujiravanit R, Supaphol P. Electrospinning of hexanoyl chitosan/polylactide blends. J Biomater Sci Polym Ed 2006;17(5):547–65.
[71] Park KE, Kang HK, Lee SJ, Min BM, Park WH. Biomimetic nanofibrous scaffolds: preparation and characterization of PGA/chitin blend nanofibers. Biomacromolecules 2006 Feb;7(2):635–43.
[72] Li L, Hsieh YL. Chitosan bicomponent nanofibers and nanoporous fibers. Carbohydr Res 2006 Feb 27;341(3):374–81.
[73] Huang L, Nagapudi K, Apkarian RP, Chaikof EL. Engineered collagen-PEO nanofibers and fabrics. J Biomater Sci Polym Ed 2001;12(9):979–93.
[74] Huang L, Apkarian RP, Chaikof EL. High-resolution analysis of engineered type I collagen nanofibers by electron microscopy. Scanning 2001 Nov–Dec;23(6):372–5.
[75] Yusof NL, Wee A, Lim LY, Khor E. Flexible chitin films as potential wound-dressing materials: wound model studies. J Biomed Mater Res A 2003 Aug 1;66(2):224–32.
[76] Kakade MV, Givens S, Gardner K, Lee KH, Chase DB, Rabolt JF. Electric field induced orientation of polymer chains in macroscopically aligned electrospun polymer nanofibers. J Am Chem Soc 2007 Mar 14;129(10):2777–82.
[77] Courtney T, Sacks MS, Stankus J, Guan J, Wagner WR. Design and analysis of tissue engineering scaffolds that mimic soft tissue mechanical anisotropy. Biomaterials 2006 Jul;27(19):3631–8.
[78] Eichhorn SJ, Sampson WW. Statistical geometry of pores and statistics of porous nanofibrous assemblies. J R Soc Interface 2005 Sep 22;2(4):309–18.
[79] Nam J, Huang Y, Agarwal S, Lannutti J. Improved cellular infiltration in electrospun fiber via engineered porosity. Tissue Eng 2007 Sep;13(9):2249–57.
[80] Pham QP, Sharma U, Mikos AG. Electrospun poly(epsilon-caprolactone) microfiber and multilayer nanofiber/microfiber scaffolds: characterization of scaffolds and measurement of cellular infiltration. Biomacromolecules 2006 Oct;7(10):2796–805.
[81] Ma Z, He W, Yong T, Ramakrishna S. Grafting of gelatin on electrospun poly(caprolactone) nanofibers to improve endothelial cell spreading and proliferation and to control cell Orientation. Tissue Eng 2005 Jul–Aug;11(7–8):1149–58.
[82] Casper CL, Yang W, Farach-Carson MC, Rabolt JF. Coating electrospun collagen and gelatin fibers with perlecan domain I for increased growth factor binding. Biomacromolecules 2007 Apr;8(4):1116–23.
[83] Lee SJ, Yoo JJ, Lim GJ, Atala A, Stitzel J. *In vitro* evaluation of electrospun nanofiber scaffolds for vascular graft application. J Biomed Mater Res A 2007 Dec 15;83(4):999–1008.
[84] Inoguchi H, Tanaka T, Maehara Y, Matsuda T. The effect of gradually graded shear stress on the morphological integrity of a huvec-seeded compliant small-diameter vascular graft. Biomaterials 2007 Jan;28(3):486–95.
[85] Zhang J, Qi H, Wang H, Hu P, Ou L, Guo S, et al. Engineering of vascular grafts with genetically modified bone marrow mesenchymal stem cells on poly (propylene carbonate) graft. Artif Organs 2006 Dec;30(12):898–905.
[86] Inoguchi H, Kwon IK, Inoue E, Takamizawa K, Maehara Y, Matsuda T. Mechanical responses of a compliant electrospun poly(L-lactide-*co*-epsilon-caprolactone) small-diameter vascular graft. Biomaterials 2006 Mar;27(8):1470–8.
[87] He W, Yong T, Teo WE, Ma Z, Ramakrishna S. Fabrication and endothelialization of collagen-blended biodegradable polymer nanofibers: potential vascular graft for blood vessel tissue engineering. Tissue Eng 2005 Sep–Oct;11(9–10):1574–88.
[88] Nie H, Soh BW, Fu YC, Wang CH. Three-dimensional fibrous PLGA/HAp composite scaffold for BMP-2 delivery. Biotechnol Bioeng 2008 Jan 1;99(1):223–34.
[89] Cui W, Li X, Zhou S, Weng J. In situ growth of hydroxyapatite within electrospun poly(DL-lactide) fibers. J Biomed Mater Res A 2007 Sep 15;82(4):831–41.
[90] Burger C, Chu B. Functional nanofibrous scaffolds for bone reconstruction. Colloids Surf B Biointerfaces 2007 Apr 15;56(1–2):134–41.
[91] Sahoo S, Ouyang H, Goh JC, Tay TE, Toh SL. Characterization of a novel polymeric scaffold for potential application in tendon/ligament tissue engineering. Tissue Eng 2006 Jan;12(1):91–9.
[92] Lee CH, Shin HJ, Cho IH, Kang YM, Kim IA, Park KD, et al. Nanofiber alignment and direction of mechanical strain affect the ECM production of human ACL fibroblast. Biomaterials 2005 Apr;26(11):1261–70.
[93] Ouyang HW, Goh JC, Thambyah A, Teoh SH, Lee EH. Knitted poly-lactide-*co*-glycolide scaffold loaded with bone marrow stromal cells in repair and regeneration of rabbit Achilles tendon. Tissue Eng 2003 Jun;9(3):431–9.
[94] Kenawy el R, Bowlin GL, Mansfield K, Layman J, Simpson DG, Sanders EH, et al. Release of tetracycline hydrochloride from electrospun poly(ethylene-*co*-vinylacetate), poly(lactic acid), and a blend. J Control Release 2002 May 17;81(1–2):57–64.
[95] Bolgen N, Vargel I, Korkusuz P, Menceloglu YZ, Piskin E. *In vivo* performance of antibiotic embedded electrospun PCL membranes for prevention of abdominal adhesions. J Biomed Mater Res B Appl Biomater 2007 May;81(2):530–43.
[96] Huang ZM, He CL, Yang A, Zhang Y, Han XJ, Yin J, et al. Encapsulating drugs in biodegradable ultrafine fibers through co-axial electrospinning. J Biomed Mater Res A 2006 Apr;77(1):169–79.
[97] Kim K, Luu YK, Chang C, Fang D, Hsiao BS, Chu B, et al. Incorporation and controlled release of a hydrophilic antibiotic using poly(lactide-*co*-glycolide)-based electrospun nanofibrous scaffolds. J Control Release 2004 Jul 23;98(1):47–56.
[98] Xu X, Chen X, Xu X, Lu T, Wang X, Yang L, et al. BCNU-loaded PEG-PLLA ultrafine fibers and their *in vitro* antitumor activity against Glioma C6 cells. J Control Release 2006 Sep 12;114(3):307–16.
[99] Xie J, Wang CH. Electrospun micro- and nanofibers for sustained delivery of paclitaxel to treat C6 glioma *in vitro*. Pharm Res 2006 Aug;23(8):1817–26.
[100] Liang D, Luu YK, Kim K, Hsiao BS, Hadjiargyrou M, Chu B. *In vitro* non-viral gene delivery with nanofibrous scaffolds. Nucleic Acids Res 2005;33(19):e170.